

APPENDIX

SUPPORTING PAPERS

1. Yu, H.M., Tseng, M.J., Fang, J.M., Phutrakul, S. and Chen, S.T. (2004) Capillary electrophoresis using immobilized whole cells with overexpressed endothelin receptor for specific ligand screening. *Electrophoresis* 25, 1034-1041.
2. Babu, G., Yu, H.M., Yang, S.M. and Fang, J.M. (2004) Carbazolothiophene-2-carboxylic acid derivatives as endothelin receptor antagonists. *Bioorg. Med. Chem. Lett.* 14, 1129-1132.
3. Wang, I., Wu, S.H., Chang, H.K., Shieh, R.C., Yu, H.M. and Chen, C. (2002) Solution structure of a K-channel blocker from the scorpion *Tityus cambridgei*. *Protein Sci.* 389-400.
4. Lee, Y.C., Lin, S.D., Yu, H.M. and Chen, S.T. (2001) Phosphorylation of the 24p3 protein secreted from mouse uterus *in vitro* and *in vivo*. *J. Protein Chem.* 20, 563-569.
5. Ho, C.L., Shih, Y.P., Wang, K.T. and Yu, H.M. (2001) Enhancing the hypotensive effect and diminishing the cytolytic activity of hornet mastoparan B by D-amino acid substitution. *Toxicon* 39, 1561-1566.
6. Yu, H.M., Lin, H.L., Wu, C.Y., Tseng, M.J. and Chen, S.T. (1999) Enzymatic reaction in supercritical fluid carbon dioxide using dry-ice. *J. Chin. Chem. Soc.* 46, 647-650.
7. Chen, S.T., Yu, H.M., and Wang, K.T. (1999) Microwave-assisted solid reaction: Reduction of ketones using sodium borohydride. *J. Chin. Chem. Soc.* 46, 509-511.
8. Yu, H.M., Chen, S.T., Tseng, M.J., Chen, S.T. and Wang, K.T. (1999) Microwave-assisted heterogeneous Benzil-Benzilic acid rearrangement. *J. Chem. Res. S*, 62-63.

Hui-Ming Yu^{1,2}
 Min-Jen Tseng³
 Jim-Min Fang⁴
 Suree Phutrakul²
 Shui-Tein Chen¹

¹Institute of Biological Chemistry,
 Academia Sinica,
 Taipei, Taiwan

²Department of Chemistry,
 Faculty of Science,
 Chiang Mai University,
 Chiang Mai, Thailand

³Graduate Institute of Cell
 and Molecular Biology,
 Taipei Medical University,
 Taipei, Taiwan

⁴Department of Chemistry,
 National Taiwan University,
 Taipei, Taiwan

Capillary electrophoresis using immobilized whole cells with overexpressed endothelin receptor for specific ligand screening

A new capillary electrophoresis method using immobilized cells as the stationary phase has been developed. The power of this method is demonstrated by the separation and identification of endothelin antagonists on a capillary column coated by the transfected Chinese hamster ovary (CHO) cells with overexpressing endothelin receptors. The screening results are validated by functional assays suppressing the increase of intracellular calcium concentration induced by endothelin-1. Instead of making efforts in isolating protein receptors, the easily prepared whole-cell capillary column provides a superior tool on the basis of ligand/receptor affinity for a rapid screening of potent drug candidates from compound libraries.

Keywords: Affinity capillary electrophoresis / Endothelin receptor antagonists / High-throughput screening / Immobilized whole cells / Receptor-ligand interaction

DOI 10.1002/elps.200305804

1 Introduction

Many biological events are triggered by ligand/receptor interactions. For example, endothelin-1 (ET-1), a 21-peptide ligand locally produced in various cell types under different physiological stimuli, has a strong affinity toward endothelin receptor A (ET_A) located on the surface of an endothelial cell membrane [1–3]. This ligand/receptor interaction is coupled with G-protein, which triggers a series of biological events to induce an increase of intracellular calcium concentration, [Ca²⁺]_i [4]. Antagonism of the endothelin vasoconstrictor is a potential approach to the treatment of a variety of human diseases including hypertension and congestive heart failure [5]. Screening of natural and synthetic compounds based on the concept of ligand/receptor recognition is an indispensable strategy to search for endothelin receptor antagonists [6–9].

Affinity capillary electrophoresis (ACE) is a powerful separation method with the advantages of high resolution, small sample requirement, rapid sample throughput, and compatibility to biological conditions [10–14]. The components in an analyte can be separated by ACE due to their different electrophoresis mobilities. By coupling with various sensitive detectors, the ACE technique is widely used to separate bioactive compounds and to determine the biomolecular noncovalent interactions [15–18]. When ACE is applied to screen active ligands in an analyte solution, the target receptor is often immobilized as the stationary phase on the inner wall of a capillary column [10–20]. However, this approach may encounter a problem in isolating of the desired receptors in sufficient quantity. Also, many membrane-bound receptors are unstable in isolation, as is the case of ET_A. Another problem is that receptors may lose their active conformations upon conjugation to capillary columns. We therefore investigated the possibility of using whole cells with overexpressing receptors, in lieu of the isolated receptors, as the stationary phase in ACE for the evaluation of active ligands [21, 22].

In this study, we demonstrate that a whole-cell stationary phase consisting of ET_A-overexpressing Chinese hamster ovary (CHO) cells provides a successful ACE protocol for the screening of the ET_A-specific ligands. The peptide and non-peptide ET_A antagonists (Fig. 1) were satisfactorily resolved on ACE, in accordance to the order of their affinity and antagonist potency toward ET_A.

Correspondence: Dr. Shui-Tein Chen, Institute of Biological Chemistry, Academia Sinica, Taipei, Taiwan
 E-mail: bcchen@gate.sinica.edu.tw
 Fax: +886-2-27883473

Abbreviations: ACE, affinity capillary electrophoresis; CHO cells, Chinese hamster ovary cells; ET_A, endothelin receptor A; ET-1, endothelin 1; ET-1^(16–21), endothelin 1 fragment containing 16–21 residues; FBS, fetal bovine serum

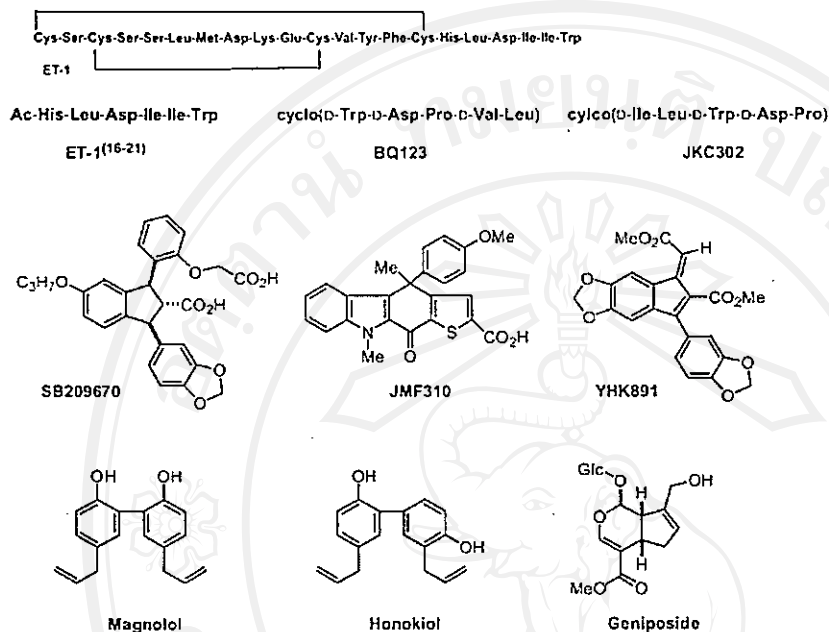


Figure 1. ET-1 and the examined substrates in this study.

2 Materials and methods

2.1 Construction of CHO-K1 cell line over-expressing ET_A and ligand-binding assay

The lipofectin-mediated transfection method described by Tseng *et al.* [23] was used to construct stable CHO cell lines overexpressing ET_A. Cells were grown to 30–40% confluence in 60 mm dishes and transfected with 1 µg of pcDNA-3 expressing plasmid harboring ET_A using lipofectin reagent for 6–8 h in serum-free medium. Cells were then returned to 5% fetal bovine serum (FBS), cultured 36 h, then replated at reduced density in 150 mm plates in the presence of 0.75 mg/mL (active) G418. G-418 resistant colonies were selected and screened for ET_A by binding of [¹²⁵I]iodotyrosyl]endothelin-1 ([¹²⁵I]ET-1). Binding was conducted to cells plated in 24-well dishes at 2–3 × 10⁵ cells/mL the day before the binding assay. For cell-binding assays, [¹²⁵I]ET-1 (10 pM) was added to HR buffer (5 mM NaCl, 4.7 mM KCl, 1 mM Na₂HPO₄, 1.28 mM CaCl₂, 10 mM HEPES, pH 7.4, with 0.5% bovine serum albumin, and 0.1 mg/mL soybean trypsin inhibitor). Cells were incubated to equilibrium (2 h at 37°C), then

washed twice with ice-cold phosphate-buffered saline. The cells were then solubilized with 1 mL of 0.1 N NaOH and radioactivity quantified in a γ-counter. Nonspecific binding was determined in the presence of 100 nM ET-1.

2.2 Preparation of a cell-immobilized capillary column

A fused-silica capillary column (60 cm effective length × 200 µm inner diameter, ~1.88 mL whole volume) was activated by washing successively with MeOH (ca. 20 mL), 1 N HCl (ca. 20 µL), deionized water (ca. 20 µL), 1 N NaOH (ca. 20 µL), and deionized water (ca. 20 µL). The column was stored in the presence of 1 mM PBS buffer (containing 31.7 mg of NaH₂PO₄ and 206 mg of Na₂HPO₄ at pH 7.3 per liter). The transfected CHO cells harboring ET_A (~2.5 × 10⁵ cells/mL) recovered from the culture media were fixed by treatment with formaldehyde (3.7% in water, 5 mL) for 30 min to furnish the desired cross-linkage. The fixed cells were stored at 4°C in PBS (1 mM, pH 7.3). For loading of the fixed cells onto the capillary column, the column was washed with EtOH (95%, ca. 40 µL), purged with air in order to dry it, charged with poly-L-lysine (15 000–

30 000 molecular weight, 0.5 mg/mL in water) for 5 min, and incubated for 30 min [24, 25]. The column was then charged again with poly-L-lysine for 5 min and incubated for 2 h. The column was then dried by airflow for 2 h, the fixed cells in the PBS buffer were purged into the poly-L-lysine-coated column. After 5 min of incubation time, another batch of fixed cells was purged into the column for 30 min of incubation. Then 1% FBS in PBS (ca. 20 μ L) was purged to cap the exposed area of poly-L-lysine. The column immobilized with the transfected CHO cells was finally washed with PBS (ca. 40 μ L), and stored at room temperature (~ 25 – 27°C). No apparent degradation was observed after 7 days. Capillary electrophoresis experiments were performed on an P/ACE system (Beckman Instruments, Fullerton, CA, USA) at a constant voltage of 10 kV. The sample (~ 1.5 μ L of $\sim 10^{-6}$ to 10^{-7} M solution in 1 mM PBS, pH 7.0) was introduced into the capillary column by pressure injection at 0.5 psi/3 s. The background electrolyte was PBS (1 mM, pH 7.0). Electrophoresis was monitored by an absorbance detector held at 214 nm. The low concentration of PBS (1 mM) ensured no interference with 214 nm absorbance. The temperature of the capillary column was maintained at 25°C .

2.3 Samples and reagents

ET-1, the ET-1 fragment ET-1^(15–21) containing 16–21 residues [26, 27], and the cyclic peptide antagonists BQ123 [28] and JKC302 [29, 30] were synthesized by using an ABI 433A peptide synthesizer (ABI, Foster City, CA, USA). We also prepared the samples of non-peptide endothelin receptor antagonists SB209670 [31, 32], JMF310 [33], and YHK891 [34]. The active herbal components, Magnolol, Geniposide and Honokiol, were purchased from Wako Pure Chemical Industries (Japan). The ^{125}I -labeled ET-1 ((3- ^{125}I iodotyrosyl)endothelin-1, 81.4 TBq/mmol) was purchased from NEN Life Science Products (Wilmington, DE, USA). The fluorescent reagent, fura-2 penta(acetoxymethyl) ester, was from Calbiochem-Novabiochem (La Jolla, CA, USA). poly-L-lysine hydrobromide and G418 antibiotic were from Sigma Chemical (St. Louis, MO, USA). All other chemicals were of analytical grade. Distilled water was used in all experiments. All buffers were filtered through 0.45 μm filters before use.

3 Results and discussion

3.1 Identification of transfected CHO cells

The cultured CHO cells were subjected to transfection with the ET_A-expression plasmid DNA using a lipofectin reagent. The efficacy of ET_A expression was demon-

strated by the competitive binding assay with a synthetic sample of ET-1 and the radiolabeled [^{125}I]-ET-1 (Fig. 2). The binding affinity of the transfected cell line by the agonist ET-1 was established to have a dissociation constant of $K_d = 1.52$ nM. The receptor density (B_{max}) of 6.3×10^5 sites/cell was estimated from a Scatchard plot [38, 39]. This result indicated that ET_A receptors were successfully overexpressed in the CHO cells. The CHO cells harboring ET_A were fixed by treatment with formaldehyde. A fused-silica capillary column (200 μm inner diameter) was first charged with poly-L-lysine, and then purged with the cross-linked CHO cells. After capping the exposed portion of poly-L-lysine with FBS, the cell-immobilized capillary column was furnished and ready for ACE. It was estimated that about 1–3 cells were attached to the capillary cross-section. Among several possible candidates of base material, poly-L-lysine turned out to exhibit a superb adhesive property for the immobilization of cells on the capillary column. The whole-cell immobilized capillary column could be easily prepared, and no obvious decomposition was found on storage with PBS buffer at room temperature for seven days.

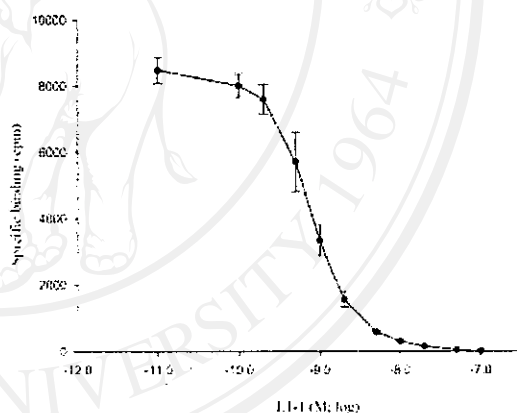


Figure 2. [^{125}I]-Endothelin-1 binding assay was performed with a synthetic endothelin-1 (ET-1). The binding affinity of transfected CHO cell-line was established with $K_d = 1.52$ nM, and B_{max} was estimated at 6.3×10^5 sites/cell.

3.2 Validation of peptide ligands

In order to validate our ACE method, we first analyzed three known peptide ligands of the ET_A receptor: an ET-1 C-terminal fragment ET-1^(15–21) containing six amino acid residues [26, 27] and two cyclic pentapeptides, BQ123 [28] and JKC302 [29, 30]. The behavior of these ligands on three different capillary columns was examined, i.e., an uncoated column, a column coated with poly-L-lysine,

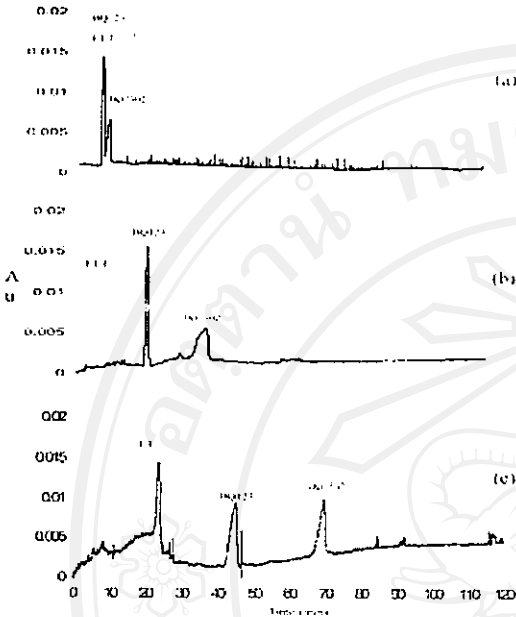


Figure 3. ACE of peptides JKC302, BQ123, and ET-1^(16–21) on a column (a) uncoated; (b) coated with poly-L-lysine; (c) coated with fixed ET_A-overexpressing CHO cells. Background electrolyte, 1 mM PBS; absorbance detector at 214 nm. Au, arbitrary unit.

and a column coated with fixed ET_A-overexpressing CHO cells. The first set of electropherograms indicated that these three compounds were poorly resolved on an uncoated column, as one would expect. The eluting order of three peptides on the poly-L-lysine-coated column differs from that on the cell-coated column, presumably due to the random electrostatic interactions exerted by poly-L-lysine on the peptide analytes. Complete separation of the mixture of ET-1^(16–21), BQ123, and JKC302 was realized on a capillary column with the stationary phase of immobilized ET_A-overexpressing CHO cells (Fig. 3). The cyclopeptide JKC302 with the longest retention time on the cell-coated column should exhibit the highest affinity toward ET_A, whereas the hexapeptide ET-1^(16–21) with the shortest retention time should have the least affinity.

The speculation of relative affinity JKC302 > BQ123 > ET-1^(16–21), as deduced from the ACE experiment, was further supported by the functional assay of their antagonistic potency against ET-1. It is well known that the binding of ET-1 with ET_A will trigger an increase of intracellular calcium concentration [4]. A control experiment (Fig. 4a) was performed by treatment of ET-1 in 10^{–7} M to the ET_A-overexpressing CHO cells, which were first incubated with a calcium-chelating agent fura-2 applied as its penta(acetoxymethyl) ester [39, 40]. The [Ca²⁺]_i change was monitored by a ratiometric method using dual excitations at 340 and 380 nm wavelengths, and the fluorescence

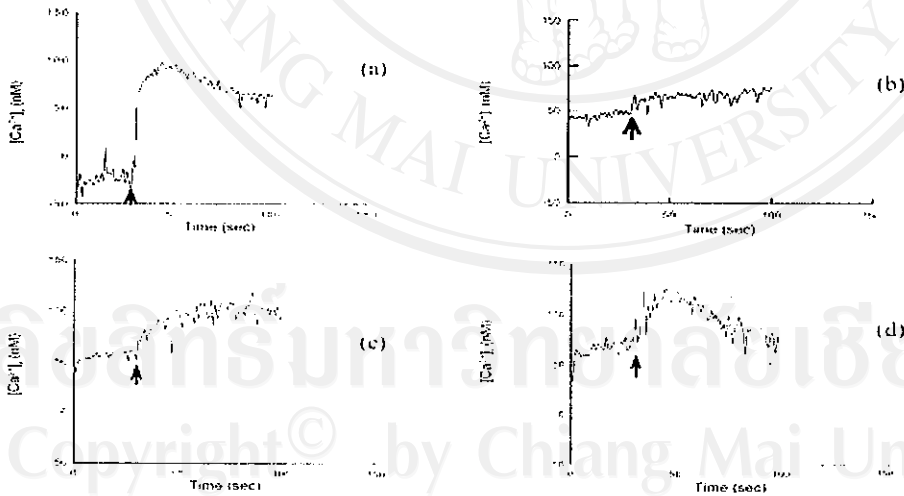


Figure 4. Fluorescence measurements of intracellular calcium concentration ([Ca²⁺]_i) by addition of tested samples (as shown by the arrow) to the ET_A-overexpressing CHO cells in the presence of fura-2. The induced [Ca²⁺]_i change is taken as a measure of antagonist potency against ET-1: (a) control experiment with addition of ET-1 (10^{–7} M), (b) treatment with a mixture of JKC302 (10^{–6} M) and ET-1 (10^{–7} M), (c) treatment with a mixture of BQ123 (10^{–6} M) and ET-1 (10^{–7} M), and (d) treatment with a mixture of ET-1^(16–21) (10^{–6} M) and ET-1 (10^{–7} M).

emission at 505 nm was measured. The treatment with ET-1 induced a great degree of $[Ca^{2+}]_i$ (Fig. 4a). When a mixture of JKC302 (10^{-6} M) and ET-1 (10^{-7} M) was used in such a functional assay, the ET-1 induced $[Ca^{2+}]_i$ change was entirely suppressed (Fig. 4b). The degree of inhibition against the ET-1 induced $[Ca^{2+}]_i$ can serve as a measure of the potency of an antagonist. By comparison of the transient $[Ca^{2+}]_i$ assays (Figs. 4b–d), the relative potency JKC302 > BQ123 > ET-1^(16–21) in ET_A antagonism is in good agreement with that derived by the eluting order on the capillary column coated with whole cells.

3.3 Validation of nonpeptide ligands

Our present whole-cell coating ACE method is not limited to peptide antagonists; it is also applicable for screening nonpeptide antagonist molecules. For example, a 1,3-diarylidene-2-carboxylic acid SB209670 is a potent ET_A antagonist against ET-1 [31]. The molecular computations together with bioassay of a series of derivatives indicated that SB209670 bears a carboxyl group at the 2-position to mimic the carboxylic terminal of ET-1, and two aryl groups at 4- and 9-positions to mimic the aromatic residues of

Tyr-13 and Phe-14. On the basis of this structural protocol, a carbazothienophene-2-carboxylic acid JMF310 [33] was designed as a possible ET_A antagonist, and an indene-carboxylate ester YHK891 [34] was also examined for comparison. Indeed, SB209670 that strongly inhibited the ET-1 induced $[Ca^{2+}]_i$ (Fig. 6b) also showed a very long retention time on the whole-cell immobilized capillary column (Fig. 5), as a consequence of its high affinity toward

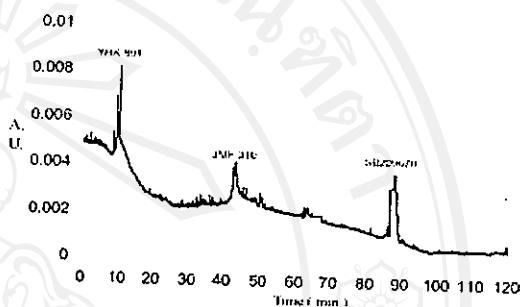


Figure 5. ACE of a mixture of SB209670, JMF310, and YHK891 on a capillary column coated with fixed ET_A-overexpressing CHO cells. Background electrolyte, 1 mM PBS; absorbance detector at 214 nm. A.U., arbitrary unit.

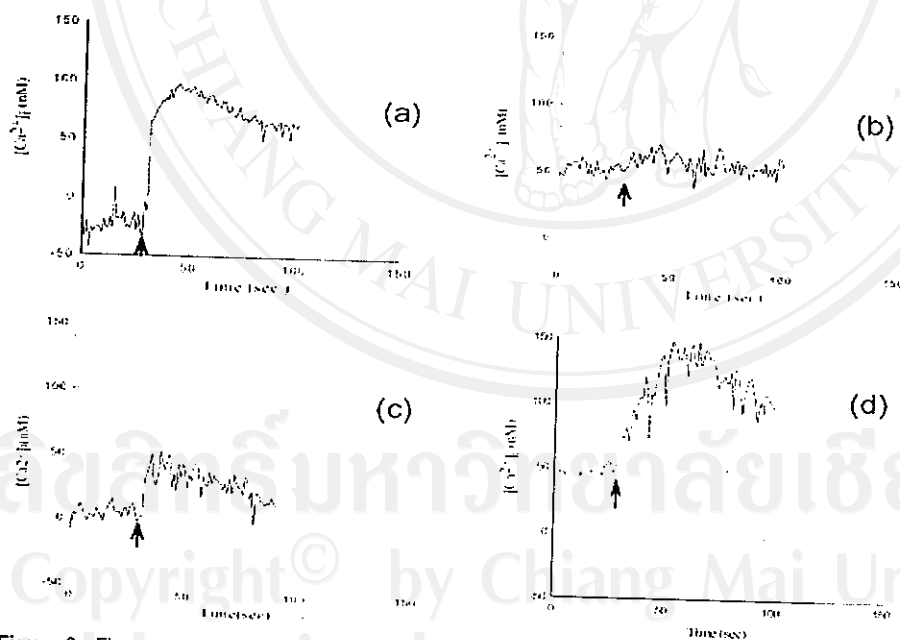


Figure 6. Fluorescence measurements of intracellular calcium concentration ($[Ca^{2+}]_i$) by addition of tested samples (as shown by the arrow) to the ET_A-overexpressing CHO cells in the presence of fura-2. The induced $[Ca^{2+}]_i$ change is taken as a measure of antagonist potency against ET-1: (a) control experiment with addition of ET-1 (10^{-7} M), (b) treatment with a mixture of SB209670 (10^{-6} M) and ET-1 (10^{-7} M), (c) treatment with a mixture of JMF310 (10^{-6} M) and ET-1 (10^{-7} M), and (d) treatment with a mixture of YHK891 (10^{-6} M) and ET-1 (10^{-7} M).

the surface endothelin receptors of the transfected CHO cells. The modest antagonist potency of JMF310 (Fig. 6c) was also reflected in the ACE elution profile. On the contrary, the YHK891 sample having only a marginal inhibitory effect against ET-1 (Fig. 6d) was rapidly eluted out from the whole-cell coating column.

3.4 Validation of active herbal components

In addition to the rationally designed molecules, the random screening of active components can also be achieved by the whole-cell ACE method. We have selected several active herbal components that are known to possess bioactivities related to vascular dilation or signal transduction. By ACE we found that an anti-platelet agent, Magnolol [42–44], might function as a new lead compound against ET-1 in ET_A receptor binding. Magnolol is the 2,2'-dimer of 4-allylphenol. As shown in the profiles of ACE analysis (Fig. 7) and $[Ca^{2+}]_i$ assay (Fig. 8), Magnolol is a stronger ET_A antagonist than its structural isomer, Honokiol [45]. Geniposide [46], an iridoid glucoside that exhibits neurotogenic effect on

PC12h cells and enhanced responses of cells to carbachol in terms of cytoplasmic free-calcium concentration, turned out to have a temperate binding affinity and modest antagonistic activity against ET-1.

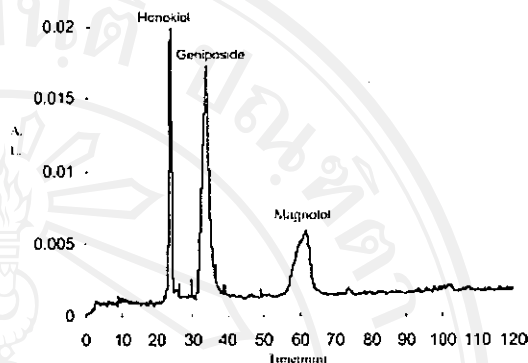


Figure 7. Screening of the Chinese herbal active components Magnolol, Honokiol, and Geniposide by ACE on a capillary column coated with fixed ET_A -overexpressing CHO cells. Background electrolyte, 1 mM PBS; absorbance detector at 214 nm. A.U., arbitrary unit.

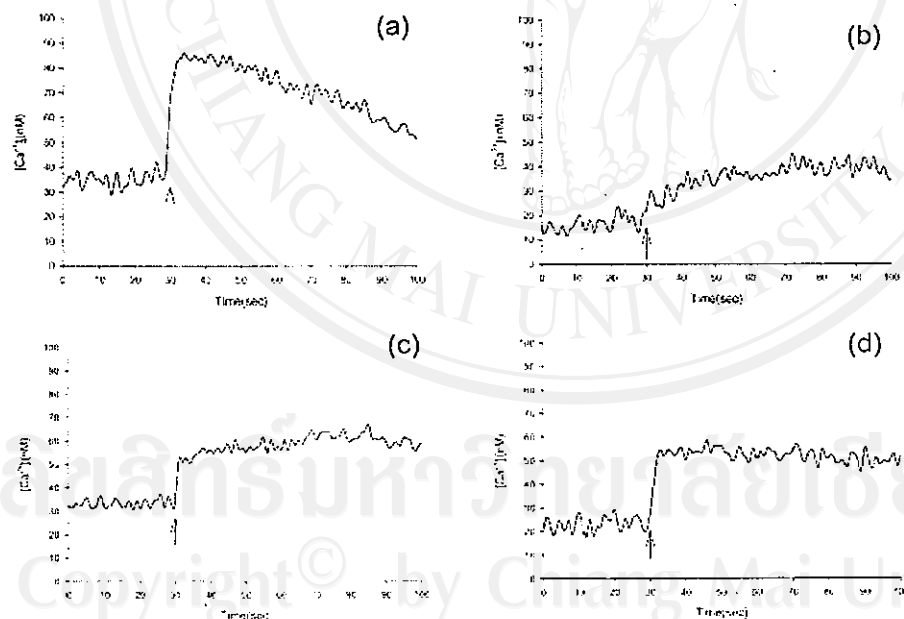


Figure 8. Fluorescence measurements of intracellular calcium concentration ($[Ca^{2+}]_i$) by addition of tested samples (as shown by the arrow) to the ET_A -overexpressing CHO cells in the presence of fura-2. The induced $[Ca^{2+}]_i$ change is taken as a measure of antagonist potency against ET-1: (a) control experiment with addition of ET-1 (10^{-7} M), (b) treatment with a mixture of Magnolol (10^{-6} M) and ET-1 (10^{-7} M), (c) treatment with a mixture of Geniposide (10^{-6} M) and ET-1 (10^{-7} M), and (d) treatment with a mixture of Honokiol (10^{-6} M) and ET-1 (10^{-7} M).

4 Concluding remarks

There are several distinct advantageous features for using whole cells as the stationary phase of ACE (i) isolation of (unstable) receptors is not needed, (ii) the stability of whole cells is improved by immobilization, and (iii) whole cells are easily coated on a fused-silica capillary column via the guidance of poly-L-lysine template. We have demonstrated this concept of whole-cell immobilized ACE by a protocol using the capillary column coated with the CHO cells harboring overexpressing endothelin receptor A. The capillary column prepared as such exhibits excellent affinity for separation and identification of endothelin receptor A antagonists (Fig. 9, Table 1). There is a good correlation between the relative inhibition of the

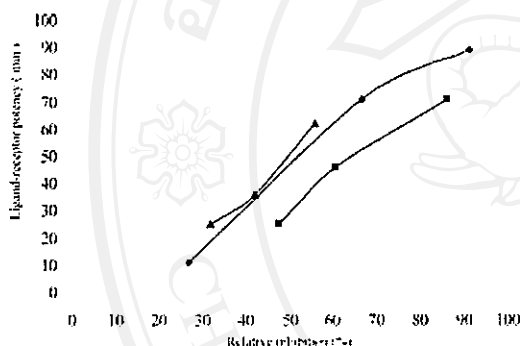


Figure 9. Correlation between the retention time of the examined compound of the capillary column coated with ET_A-overexpressing CHO cells and the relative inhibition of the ET-1 induced increase of intracellular calcium ion concentration. In each line, the stronger affinity of a compound toward ET_A shows a longer retention time and more potent inhibitory effect. (■) From top to bottom are JKC302, BQ123, and ET-1^(16–21); (◆) from top to bottom are SB209670, JMF310, and YHK891; (▲) from top to bottom are Magnolol, Geniposide, and Honokiol.

Table 1. Relative inhibition of the ET-1 induced [Ca²⁺]_i and retention time of the examined compound on the capillary column coated with ET_A-overexpressing CHO cells

Compound	Relative inhibition (%)	Retention time (min)
JKC302	86	69.7
BQ123	61	45.0
ET-1 ^(16–21)	48	24.2
SB209670	91	87.8
JMF310	67	69.7
YHK891	27	10.0
Magnolol	56	61.4
Geniposide	42	34.7
Honokiol	32	24.1

ET-1 induced [Ca²⁺]_i and the retention time of the examined compound on the capillary column coated with ET_A-overexpressing CHO cells. This ACE method only requires a small quantity of sample, and offers a reliable assessment of a library of compounds in a relatively short period. The ACE with immobilized whole cells could be developed as a high-throughput screening method based on specific receptor/ligand interactions.

The authors like to thank Prof. Yueh-Hsiung Kuo and Yeun-Min Tsai (Department of Chemistry, National Taiwan University) for kindly providing us the samples of YHK891 and SB209670 and Prof. Sheau-Huei Chueh (Department of Biochemistry, National Defense University) for directing us the [Ca²⁺]_i assay. We also thank the National Science Council and Taipei Medical University (TMC 87-Y05-A128 to M.-J. T.) for financial support. Support for the research (S.-T. Chen) provided by the Main Subject Projects of Academia Sinica, Taiwan and the National Research Program for Genomic Medicine, National Science Council, Taiwan, (NSC 91-3112-13-001-002) are greatly appreciated.

Received September 28, 2003

5 References

- [1] Yanagisawa, M., Kurihara, H., Kimura, S., Tomobe, Y., Kobayashi, M., Mitsui, Y., Yazaki, Y., Goto, K., Masaki, T., *Nature* 1988, 332, 311–315.
- [2] Doherty, A. M., *J. Med. Chem.* 1992, 35, 1493–1508.
- [3] Schiffrin, E. L., Touyz, R. M., *J. Cardiovasc. Pharmacol.* 1998, 32, Suppl. 3, 2–13.
- [4] Sakurai, T., Yanagisawa, M., Masaki, T., *Trends Pharmacol. Sci.* 1992, 13, 103–108.
- [5] Lerman, A., *J. Cardiovasc. Pharmacol.* 2001, 38, Suppl. 2, 27–30.
- [6] Elliott, J. D., Lago, M. A., Peishoff, C. E., in: Ruffolo, R. R. (Ed.), *Endothelin Receptors: From the Gene to the Human*, CRC Press, Boca Raton, FL 1995, pp. 79–107.
- [7] Doherty, A. M., *Drug Discovery Today* 1996, 1, 60–70.
- [8] Webb, M. L., Meek, T. D., *Med. Res. Rev.* 1997, 17, 17–67.
- [9] Liu, G., *Annu. Rev. Med. Chem.* 2000, 35, 73–82.
- [10] Fishman, H. A., Orwar, O., Scheller, R. H., Zare, R. N., *Proc. Natl. Acad. Sci. USA* 1995, 92, 7877–7881.
- [11] Chu, Y. H., Dunayevskiy, Y. M., Kirby, D. P., Vouros, P., Karger, B. L., *J. Am. Chem. Soc.* 1996, 118, 7827–7835.
- [12] Landers, J. P. (Ed.), *Handbook of Capillary Electrophoresis*, 2nd ed., CRC Press, Boca Raton, FL 1997, pp. 591–609.
- [13] Chu, Y. H., Cheng, C. C., *Cell Mol. Life Sci.* 1998, 54, 663–683.
- [14] Yeung, E. S., *J. Chromatogr. A* 1999, 830, 243–262.
- [15] Colton, I. J., Carbeck, J. D., Rao, J., Whitesides, G. M., *Electrophoresis* 1998, 19, 367–382.
- [16] Chu, Y.-H., Zang, X., Tu, J., *J. Chin. Chem. Soc.* 1998, 45, 713–720.
- [17] Mito, E., Zhang, Y., Esquivel, S., Gomez, F. A., *Anal. Biochem.* 2000, 280, 209–215.

- [18] Kaddis, J., Mito, E., Heintz, J., Plazas, A., Gomez, F. A., *Electrophoresis* 2003, 24, 1105–1110.
- [19] Kaufman, S. E., Brown, S., Stauber, G. B., *Anal. Biochem.* 1993, 211, 261–266.
- [20] Oda, Y., Owa, T., Sato, T., Boucher, B., Daniels, S., Yamana, H., Shinohara, Y., Yokoi, A., Kuromitsu, J., Nagasu, T., *Anal. Chem.* 2003, 75, 2159–2165.
- [21] Fishman, H. A., Orwar, O., Alibritton, N. L., Modi, B. P., Shear, J. B., Scheller, R. H., Zare, R. N., *Anal. Chem.* 1996, 68, 1181–1186.
- [22] Miller, K. J., Lytle, F. E., *Anal. Chem.* 1994, 66, 2420–2423.
- [23] Tseng, M.-J., Detjen, K., Struk, V., Logsdon, C. D., *J. Biol. Chem.* 1995, 270, 18858–18864.
- [24] Leif, R. C., Ingram, D., Clay, C., Bobbitt, D., Gaddis, R., Leif, S. B., Nordqvist, S., *J. Histochem. Cytochem.* 1977, 25, 538–543.
- [25] Viekling, U., Swierenga, S. H., *Histochemistry* 1989, 91, 81–88.
- [26] Kimura, S., Kasuya, Y., Sawamura, T., Shinmi, O., Sugita, Y., Yanagisawa, M., Goto, K., Masaki, T., *Biochem. Biophys. Res. Commun.* 1988, 156, 1182–1186.
- [27] Hashido, K., Gamou, T., Adachi, M., Tabuchi, H., Watanabe, T., Furuichi, Y., Miyamoto, C., *Biochem. Biophys. Res. Commun.* 1992, 187, 1241–1248.
- [28] Ishikawa, K., Fukami, T., Nagase, T., Fujita, K., Hayama, T., Niyama, K., Mase, T., Ihara, M., Yano, M., *J. Med. Chem.* 1992, 35, 2139–2144.
- [29] Miyata, S., Hashimoto, M., Fujie, K., Nishikawa, M., Kiyoto, S., Okuhara, M., Kohsaka, M., *J. Antibiot.* 1992, 45, 83–87.
- [30] Miyata, S., Fukami, N., Neya, M., Takase, S., Kiyoto, S., *J. Antibiot.* 1992, 45, 788–791.
- [31] Elliott, J. D., Lago, M. A., Cousins, R. D., Gao, A., Leber, J. D., Erhard, K. F., Nambi, P., Elshourbagy, N. A., Kumar, C., Lee, J. A., Bean, J. W., DeBrosse, C. W., Eggleston, D. S., Brooks, D. P., Feuerstein, G., Ruffolo, R. R., Weinstein, J., Gleason, J. G., Peishoff, C. E., Ohlstein, E. H., *J. Med. Chem.* 1994, 37, 1553–1557.
- [32] Clark, W. M., Tickner-Eldridge, A. M., Huang, G. K., Pridgen, L. N., Olsen, M. A., Mills, R. J., Lantos, I., Baine, N. H., *J. Am. Chem. Soc.* 1998, 120, 4550–4551.
- [33] Babu, G., Yu, H.-M., Yang, S.-M., Fang, J.-M., *Bioorg. Med. Chem. Lett.* 2004, 14, 1129–1132.
- [34] Kuo, Y.-H., Wu, C.-H., Wu, R.-E., Lin, S.-T., *Chem. Pharm. Bull.* 1995, 43, 1267–1271.
- [35] Arai, H., Hori, H., Aramori, I., Ohkubo, H., Nakanishi, S., *Nature* 1990, 348, 730–732.
- [36] Sakurai, T., Yanagisawa, M., Takawa, Y., Miyazaki, H., Kimura, S., Goto, K., Masaki, T., *Nature* 1990, 348, 732–735.
- [37] Sakamoto, A., Yanagisawa, M., Tsujimoto, G., Nakao, K., Toyooka, T., Masaki, T., *Biochem. Biophys. Res. Commun.* 1994, 200, 679–686.
- [38] Fischli, W., Clozel, M., Guilly, C., *Life Sci.* 1989, 44, 1429–1436.
- [39] Waeber, C., Hoyer, D., Palacios J. M., *Eur. J. Pharmacol.* 1991, 176, 233–236.
- [40] Gryniewicz, G., Poenie, M., Tsien, R. Y., *J. Biol. Chem.* 1985, 260, 3440–3450.
- [41] Lin, W.-W., Chuang, D. M., *Mol. Pharmacol.* 1993, 44, 158–165.
- [42] Teng, C. M., Chen, C. C., Ko, F. N., Lee, L. G., Huang, T. F., Chen, Y. P., Hsu, H. Y., *Thrombosis Res.* 1988, 50, 757–765.
- [43] Hamasaki, Y., Kobayashi, I., Zaitu, M., Tsuji, K., Kita, M., Hayasaka, R., Muro, E., Yamamoto, S., Matsuo, M., Ichimaru, T., Miyazaki, S., *Planta Med.* 1999, 65, 222–226.
- [44] Chen, Y.-H., Lin, S.-J., Chen, J.-W., Ku, H.-H., Chen, Y.-L., *Brit. J. Pharmacol.* 2002, 135, 37–47.
- [45] Park, E. J., Zhao, Y. Z., Na, M. K., Bae, K. H., Kim, Y. H., Lee, B. H., Sohn, D. H., *Planta Med.* 2003, 69, 33–37.
- [46] Yamazaki, M., Chiba, K., Mohri, T., *Biol. Pharm. Bull.* 1996, 19, 791–795.

ลิขสิทธิ์มหาวิทยาลัยเชียงใหม่
Copyright© by Chiang Mai University
All rights reserved



Carbazolothiophene-2-carboxylic acid derivatives as endothelin receptor antagonists

Govindarajulu Babu,^a Hui-Ming Yu,^{b,c} Shyh-Ming Yang^a and Jim-Min Fang^{a,d,*}

^aDepartment of Chemistry, National Taiwan University, Taipei, 106, Taiwan

^bInstitute of Biochemistry, Academia Sinica, Taipei, 115, Taiwan

^cDepartment of Chemistry, Faculty of Science, Chiang Ma University, Thailand

^dGenomic Research Center, Academia Sinica, Taipei, 115, Taiwan

Received 14 November 2003; revised 17 December 2003; accepted 18 December 2003

Abstract—The SmI_2 -promoted three-component coupling reaction of thiophene-2-carboxylate, indole-2-carbaldehyde and acetophenone provides an expedient route to a series of tetracyclic carbazolothiophene compounds bearing the indole and thiophene rings. Among these samples, 9-benzyl-4-methyl-4-(4-hydroxyphenyl)-10-oxo-4,10-dihydrocarbazolo[2,3-*b*]thiophene-2-carboxylic acid (**18**) shows the most potent inhibition against the endothelin-1 induced increase of intracellular calcium ion concentration. © 2003 Elsevier Ltd. All rights reserved.

Human endothelin-1 (ET-1) is a 21 amino acid peptide that exhibits a potent vasoconstrictor activity, conceivably through its selective interaction with specific receptor subtypes (ET_A , ET_B and ET_C).¹ ET-1 contains six highly conserved amino acid residues (His¹⁶-Trp²¹) at the C-terminus, and this hydrophobic C-terminal hexapeptide alone shows some affinity for ET_A receptor. Several antagonists including BQ123 [cyclo(L-Leu-D-Val-L-Pro-D-Asp-D-Trp)]² are designed on the basis of this peptide structures that incorporate indole moieties. Some non-peptide endothelin antagonists also consist of indole scaffolds such as the indole-2-carboxylic acids PD159433³ and SB209598⁴ (Fig. 1). On the other hand, the molecular modeling indicates that an indan derivative SB209670⁵ possesses two phenyl substituents to mimic the amino acid residues of Trp-13 and Phe-14 in ET-1. The two carboxylic groups in SB209670 also mimic the Asp-18 residue and the C-terminus of ET-1, which ligate Zn^{2+} ion on binding with endothelin receptor.¹ We speculated that a new class of carbazolothiophene derivatives (e.g., 7–22) bearing appropriate substituents might serve as endothelin receptor antagonists. Indeed, 5-benzyloxy-3-isopropoxy-benzothiophene-2-carboxylic acid^{3,6} has been utilized as a lead com-

pound for development of endothelin antagonists. A thiophene-3-sulfonamide TBC11251⁷ is also known as an ET_A -selective antagonist, in which the sulfonamide moiety is considered an isostere of carboxylic acid. We are thus interested in applying our established method of three-component coupling reactions of thiophene-2-carboxylate⁸ to synthesize carbazolothiophene-2-

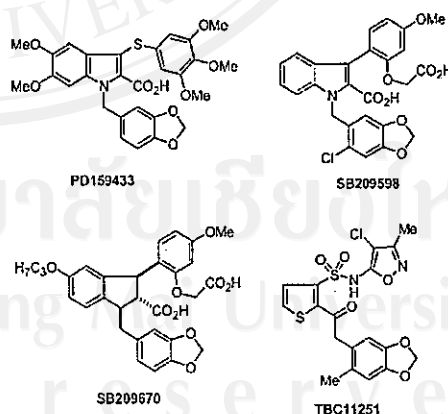


Figure 1. Some representative endothelin receptor antagonists constructed by the indole, indan and thiophene scaffolds.

Keywords: Coupling reactions; Endothelin; Samarium diiodide; Thiophene; Indole.

* Corresponding author. Tel.: +1-8862-23637812; fax: +1-8862-23636359; e-mail: jmfang@ntu.edu.tw

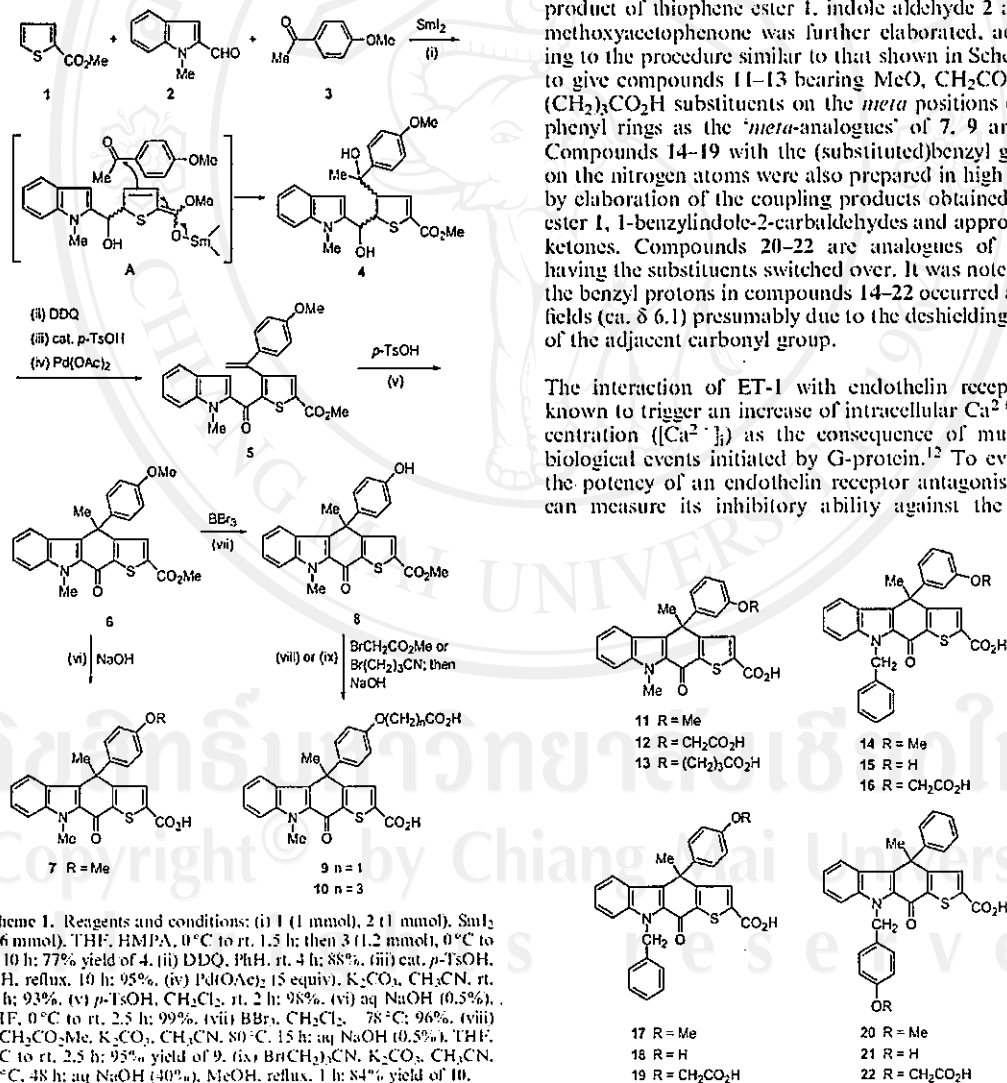
carboxylate derivatives 7–22, and examined their antagonism against the binding of ET-1 with ET_A receptor.

By the promotion of samarium diiodide, the three-component coupling reaction of methyl thiophene-2-carboxylate (1) with *N*-methylindole-2-carbaldehyde (2) and 4-methoxyacetophenone (3) occurred smoothly to afford a 77% yield of 4 (Scheme 1).^{9,10} This one-pot operation presumably proceeded by an initial coupling of ester 1 with aldehyde 2 to give a dienolate intermediate A,^{8,11} which was then trapped by ketone 3. Although diol 4 existed as a mixture of diastereomers, the subsequent oxidation and dehydration would yield a single product. Conversion of 4 to 5 was achieved by a three-step sequence: an oxidation with DDQ to give the

corresponding ketone, an acid-catalyzed dehydration to eliminate a water molecule, and an oxidative aromatization by using Pd(OAc)₂ to afford the thiophene product 5. The subsequent intramolecular Friedel-Crafts alkylation thus furnished the tetracyclic skeleton, giving carbazothienophene-2-carboxylate 6 as a pivotal compound for the synthesis of other derivatives 7–10. Saponification of 6 afforded acid 7, whereas demethylation of 6 with BBr₃ gave phenol 8. Alkylation of phenol 8 with methyl 2-bromoacetate or 4-bromobutanenitrile, followed by hydrolysis in alkaline conditions, gave diacids 9 and 10 in high yields.

A series of carbazothienophenes 11–22 were similarly prepared, initially by the SmI₂-promoted three-component coupling reactions with appropriate partner substrates. For example, the SmI₂-promoted coupling product of thiophene ester 1, indole aldehyde 2 and 3-methoxyacetophenone was further elaborated, according to the procedure similar to that shown in Scheme 1, to give compounds 11–13 bearing MeO, CH₂CO₂H or (CH₂)₃CO₂H substituents on the *meta* positions of the phenyl rings as the '*meta*-analogues' of 7, 9 and 10. Compounds 14–19 with the (substituted)benzyl groups on the nitrogen atoms were also prepared in high yields by elaboration of the coupling products obtained from ester 1, 1-benzylindole-2-carbaldehydes and appropriate ketones. Compounds 20–22 are analogues of 17–19 having the substituents switched over. It was noted that the benzyl protons in compounds 14–22 occurred at low fields (ca. δ 6.1) presumably due to the deshielding effect of the adjacent carbonyl group.

The interaction of ET-1 with endothelin receptor is known to trigger an increase of intracellular Ca²⁺ concentration ([Ca²⁺]_i) as the consequence of multistep biological events initiated by G-protein.¹² To evaluate the potency of an endothelin receptor antagonist, one can measure its inhibitory ability against the ET-1



induced $[Ca^{2+}]_i$ change. According to the reported experimental protocol,¹³ Chinese hamster ovary (CHO-K1) cells were transfected with the rat ET_A -expression plasmid DNA using lipofectin reagent (Life Technologies Inc., USA). The ET_A overexpression CHO-K1 cells were prior incubated with calcium chelating agent fura-2 applied as its penta(acetoxymethyl) ester,¹⁴ and then treated with ET-1 in 10^{-7} M. The $[Ca^{2+}]_i$ increase was monitored at 510-nm fluorescence emission by a ratio-metric method using dual excitations at 340 and 380 nm wavelengths.¹³ This increment of functional assay was taken as the standard value (100%) to assess the inhibitory potency of compounds 7–22 against the ET-1 binding with receptor. On addition of the test sample 7 (10^{-6} M) along with ET-1 (10^{-7} M), only $30 \pm 5\%$ increment of $[Ca^{2+}]_i$ was observed (a mean value of three measurements), equivalent to $\sim 70\%$ inhibition. By comparisons with the known ET_A antagonists, 10^{-6} M of SB209670 completely inhibited the ET-1 induced $[Ca^{2+}]_i$, whereas BQ123 showed $\sim 60\%$ inhibition under our assay conditions. Accordingly, compounds 9, 10, 12, 13 and 18 showed high inhibition ($> 75\%$) at 10^{-6} M. Compounds 7, 11, 15 and 19 showed medium inhibition (50–70%), whereas compounds 14, 16, 17 and 20–22 showed low inhibition. Among our examined samples, compound 18 appeared to be the best ET-1 antagonist with $IC_{50} \sim 10$ nM. In comparison, SB209670 is an even more potent antagonist showing $\sim 85\%$ inhibition at 10 nM.

In summary, a series of tetracyclic compounds 7–22 bearing the indole and thiophene rings were prepared in an expedient fashion. The functional assay indicated that one of these samples (compound 18) can serve as a lead compound for future exploration of potent endothelin receptor antagonists. The structure activity relationship also awaits further investigation.

Acknowledgements

The authors like to thank Prof. Wan-Wan Lin (Department of Pharmacology, National Taiwan University) and Sheau-Huei Chueh (Department of Biochemistry, National Defence University) for instructing us $[Ca^{2+}]_i$ assay. We also thank National Science Council for financial support.

References and notes

- (a) For biological role of endothelins, see: Yanagisawa, M.; Kurihara, H.; Kimura, S.; Tomobe, Y.; Kobayashi, M.; Mitsui, Y.; Yazaki, Y.; Goto, K.; Masaki, T. *Nature* 1988, 332, 311. (b) Doherty, A. M. *J. Med. Chem.* 1992, 35, 1493. (c) Schiffrin, E. L.; Touyz, R. M. *J. Cardiovasc. Pharmacol.* 1998, 32 (Suppl. 3), 2. (d) For review of endothelin antagonists, see: Elliott, J. D.; Lago, M. A.; Peishoff, C. E. *Endothelin Receptors: from the Gene to the Human*, Ruffolo, R. R., Ed.; CRC: Boca Raton, Florida, 1995; p 79. (e) Doherty, A. M. *Drug Discovery Today* 1996, 1, 60. (f) Webb, M. L.; Meek, T. D. *Med. Res. Rev.* 1997, 17, 17. (g) Liu, G. *Annu. Rep. Med. Chem.* 2000, 35, 73.
- Ishikawa, K.; Fukami, T.; Nagase, T.; Fujita, K.; Hayama, T.; Niyama, K.; Mase, T.; Ihara, M.; Yano, M. *J. Med. Chem.* 1992, 35, 2139.
- Bunker, A. M.; Edmunds, J. J.; Berryman, K. A.; Walker, D. M.; Flynn, M. A.; Welch, K. M.; Doherty, A. M. *Bioorg. Med. Chem. Lett.* 1996, 6, 1367.
- Elliott, J. D.; Leber, J. D. *PCT Int. Appl.* 1994, 48 pp WO 9414434 A1 19940707.
- (a) Elliott, J. D.; Lago, M. A.; Cousins, R. D.; Gao, A.; Leber, J. D.; Erhard, K. F.; Nambi, P.; Elshourbagy, N. A.; Kumar, C.; Lee, J. A.; Beam, J. W.; DeBrosse, C. W.; Eggleston, D. S.; Brooks, D. P.; Feuerstein, G.; Ruffolo, R. R.; Weinstein, J.; Gleason, J. G.; Peishoff, C. E.; Ohlstein, E. H. *J. Med. Chem.* 1994, 37, 1553. (b) Clark, W. M.; Trickner-Eldridge, A. M.; Huang, G. K.; Pridgen, L. N.; Olsen, M. A.; Mills, R. J.; Santos, L.; Baine, N. H. *J. Am. Chem. Soc.* 1998, 120, 4550.
- Bunker, A. M.; Edmunds, J. J.; Berryman, K. A.; Walker, D. M.; Flynn, M. A.; Welch, K. M.; Doherty, A. M. *Bioorg. Med. Chem. Lett.* 1996, 6, 1061.
- (a) Wu, C.; Chan, M. F.; Stavros, F.; Raju, B.; Okun, I.; Mong, S.; Keller, K. M.; Brock, T.; Kogan, T. P.; Dixon, R. A. F. *J. Med. Chem.* 1997, 40, 1690. (b) Wu, C.; Decker, E. R.; Holland, G. W.; Brown, P. M.; Stavros, F. D.; Brock, T. A.; Dixon, R. A. F. *Drugs of Today* 2001, 37, 441.
- (a) Yang, S.-M.; Fang, J.-M. *Tetrahedron Lett.* 1997, 38, 1589. (b) Yang, S.-M.; Shie, J.-J.; Fang, J.-M.; Nandy, S. K.; Chang, H.-Y.; Lu, S.-H.; Wang, G. *J. Org. Chem.* 2002, 67, 5208.
- Representative procedure for the SmI_2 promoted three-component coupling reactions: Under an atmosphere of argon, a deep blue SmI_2 solution (0.1 M) was prepared by treatment of Sm (661 mg, 4.4 mmol) with 1,2-diodoethane (1.01 g, 3.6 mmol) in HMPA¹⁰ (2.8 mL, 16 mmol) and anhydrous THF (32 mL) for 1.5 h at room temperature. To the SmI_2 solution (cooled in an ice bath) were added a THF solution (3 mL) of methyl thiophene-2-carboxylate (142 mg, 1 mmol) and *N*-methylindole-2-carbaldehyde (159 mg, 1 mmol). The reaction mixture was stirred at 0°C for 45 min, and then at room temperature (27°C) for 45 min. A THF solution (2 mL) of 4-methoxyacetophenone (180 mg, 1.2 mmol) was added at 0°C, and the mixture was stirred at 0–27°C for additional 10 h. The reaction was quenched by addition of saturated aqueous NH_4Cl solution (0.1 mL). The mixture was passed through a short silica gel column by rinse with EtOAc:hexane (1:1). The filtrate was concentrated, and chromatographed on a silica gel column by elution with EtOAc:hexane (3:7) to give the desired three-component coupling product 4 (349 mg, 77%) as a mixture of isomers as shown by the 1H NMR analysis. Compounds 5–22 were fully characterized by spectroscopic methods (IR, MS, HRMS, 1H and ^{13}C NMR) and elemental analyses. Some pertinent data are listed. 5: 1H NMR (300 MHz, $CDCl_3$) δ 7.83 (s, 1H), 7.59 (d, 1H, $J=8.0$ Hz), 7.35 (t, 1H, $J=8.0$ Hz), 7.24 (d, 1H, $J=8.0$ Hz), 7.11 (t, 1H, $J=8.0$ Hz), 6.99 (s, 1H), 6.82 (d, 2H, $J=8.5$ Hz), 6.59 (d, 2H, $J=8.5$ Hz), 5.34 (s, 1H), 5.33 (s, 1H), 3.92 (s, 3H), 3.70 (s, 3H), 3.57 (s, 3H). 6: mp 113–114°C; 1H NMR (400 MHz, $CDCl_3$) δ 7.54 (s, 1H), 7.42 (m, 2H), 7.25 (m, 3H), 7.01 (m, 1H), 6.79 (dd, 2H, $J=6.8, 2.0$ Hz), 4.28 (s, 3H), 3.86 (s, 3H), 3.74 (s, 3H), 2.09 (s, 3H). 7: mp $> 300^\circ C$. 8: mp 251–252°C. 9: mp 211–212°C. 10: mp 261–262°C. 11: mp 241–242°C. 12: mp 259–260°C. 13: mp 271–272°C. 14: mp 263–264°C. 15: mp 162–163°C. 16: mp 149–150°C. 17: mp 286–288°C. 18: mp 307–308°C. 1H NMR (400 MHz, CD_3COCD_3) δ 7.61 (s, 1H), 7.58 (dd, 1H, $J=8.4, 1.2$ Hz), 7.35–7.18 (m, 9H), 7.02 (dt, 1H, $J=7.6,$

- 0.8 Hz), 6.78 (td, 2H, $J=8.8, 3.2$ Hz), 6.16 (d, 1H, $J=16.0$ Hz), 6.11 (d, 1H, $J=16.0$ Hz), 2.19 (s, 3H), 19; mp 244–245°C, 20; mp 217–218°C, 21; mp 291–292°C, 22; mp 150–151°C.
10. (a) For use of hexamethylphosphoramide (HMPA) as a general additive to samarium diiodide in reaction acceleration and regiochemical control, see: Inanaga, J.; Ishikawa, M.; Yamaguchi, H. *Chem. Lett.* 1987, 1485. (b) Shiue, J.-S.; Lin, C.-C.; Fang, J.-M. *Tetrahedron Lett.* 1993, 34, 335.
 11. Nakayama, J.; Sugino, M.; Ishii, A.; Hoshino, M. *Chem. Lett.* 1992, 703.
 12. Sakurai, T.; Yanagisawa, M.; Masaki, T. *Trends Pharmacol. Sci.* 1992, 13, 103.
 13. (a) Arai, H.; Hori, H.; Aramori, I.; Ohkubo, H.; Nakanishi, S. *Nature* 1990, 348, 730. (b) Sakurai, T.; Yanagisawa, M.; Takuwa, Y.; Miyazaki, H.; Kimura, S.; Goto, K.; Masaki, T. *Nature* 1990, 348, 732. (c) Sakamoto, A.; Yanagisawa, M.; Tsujimoto, G.; Nakao, K.; Toyooka, T.; Masaki, T. *Biochem. Biophys. Res. Commun.* 1994, 200, 679.
 14. (a) Grynkiewicz, G.; Poenie, M.; Tsien, R. Y. *J. Biol. Chem.* 1985, 260, 3440. (b) Lin, W.-W.; Chuang, D. M. *Mol. Pharmacol.* 1993, 44, 158.

Solution structure of a K⁺-channel blocker from the scorpion *Tityus cambridgei*

IREN WANG,^{1,2} SHIH-HSIUNG WU,^{2,3} HSUEH-KAI CHANG,¹ RU-CHI SHIEH,¹ HUI-MING YU,³ AND CHINPAN CHEN¹

¹Institute of Biomedical Sciences, Academia Sinica, Taipei 115, Taiwan

²Institute of Biochemical Sciences, National Taiwan University, Taipei 106, Taiwan

³Institute of Biological Chemistry, Academia Sinica, Taipei 115, Taiwan

(RECEIVED August 9, 2001; FINAL REVISION October 17, 2001; ACCEPTED November 9, 2001)

Abstract

A new K⁺-channel blocking peptide identified from the scorpion venom of *Tityus cambridgei* (Te1) is composed of 23 amino acid residues linked with three disulfide bridges. Te1 is the shortest known toxin from scorpion venom that recognizes the *Shaker* B K⁺ channels and the voltage-dependent K⁺ channels in the brain. Synthetic Te1 was produced using solid-phase synthesis, and its activity was found to be the same as that of native Te1. The pairings of three disulfide bridges in the synthetic Te1 were identified by NMR experiments. The NMR solution structures of Te1 were determined by simulated annealing and energy-minimization calculations using the X-PLOR program. The results showed that Te1 contains an α -helix and a 3_{10} -helix at N-terminal Gly⁴–Lys¹⁰ and a double-stranded β -sheet at Gly¹³–Ile¹⁶ and Arg¹⁹–Tyr²³, with a type I' β -turn at Asn¹⁷–Gly¹⁸. Superposition of each structure with the best structure yielded an average root mean square deviation of 0.26 ± 0.05 Å for the backbone atoms and of 1.40 ± 0.23 Å for heavy atoms in residues 2 to 23. The three-dimensional structure of Te1 was compared with two structurally and functionally related scorpion toxins, charybdotoxin (ChTx) and noxiustoxin (NTx). We concluded that the C-terminal structure is the most important region for the blocking activity of voltage-gated (Kv-type) channels for scorpion K⁺-channel blockers. We also found that some of the residues in the larger scorpion K⁺-channel blockers (31 to 40 amino acids) are not involved in K⁺-channel blocking activity.

Keywords: Scorpion venom; α -KTx; K⁺-channel blocker; NMR; structure

Ion channels are involved in diverse biological processes and play essential roles in the physiology of all cells. An increasing number of human and animal diseases have been identified as relating to the defective function of ion chan-

nels. Scorpion venoms contain various polypeptides with distinct biological functions that particularly affect the permeability of ion channels in cell membranes (Catterall 1980; Valdivia et al. 1992; Garcia et al. 1997). These polypeptides possess the potency to recognize ion channels and receptors in excitable membranes and are classified into four groups on the basis of ion-channel types: (1) group I modulates Na⁺-channel activity (Possani et al. 1999) and contains peptides of 60 to 70 amino acids linked by four disulfide bridges; (2) group II blocks K⁺ channels (Miller 1995; Romi-Lebrun et al. 1997) and are short peptides with 31 to 41 amino acid residues with three or four disulfide bonds; (3) group III supposedly inhibits Cl⁻ channels (De-Bin et al. 1993) and contains short-chain insect toxin peptides of ~36 amino acids with four disulfide bonds; and (4) group IV includes peptides that modulate ryanodine-sensitive Ca²⁺ channels (Valdivia and Possani 1998). It is believed that the toxin has a unique tertiary structure that may

Reprint requests to: Chinpan Chen, Institute of Biomedical Sciences, Academia Sinica, Taipei 115, Taiwan; e-mail: bmcchen@ccvax.sinica.edu.tw; fax: 886-2-2788-7641 or Shih-Hsiung Wu, Institute of Biological Chemistry, Academia Sinica, Taipei 115, Taiwan; e-mail: shwu@gate.sinica.edu.tw; fax: 886-2-2653-9142.

Abbreviations: Te1, a new scorpion toxin from *Tityus cambridgei*; NTx, noxiustoxin; ChTx, charybdotoxin; KTx, labrotoxin; MgTx, margatoxin; IbTx, iberitoxin; TsTx-Ka, tityustoxin K- α ; BK_{Ca}, large-conductance calcium-activated potassium channel; Kv, *Shaker*-related voltage-gated potassium channel; CD, circular dichroism; NOE, nuclear Overhauser enhancement; DQF-COSY, double-quantum-filtered scalar-correlated spectroscopy; TOCSY, total correlation spectroscopy; RMSD, root mean square deviation; CSI, chemical shift index.

Article and publication are at <http://www.protein-science.org/cgi/doi/10.1110/p.33402>.

provide valuable information for understanding channels. Thus, understanding the structural basis of the specificity of scorpion toxins for these receptors could lead to the design of new ligands with controlled activity and potency with potential for clinical applications.

Scorpion K⁺-channel blockers of group II, named α -KTx, have been classified into 12 subfamilies (Miller 1995; Tytgat et al. 1999). These K⁺-channel blockers block two major classes of K⁺ channels: voltage-gated (Kv-type) and high-conductance Ca²⁺-activated (BK-type) K⁺ channels. The three-dimensional structures of several scorpion K⁺-channel blockers have been determined by NMR spectroscopy: these include charybdotoxin (ChTx; Bontems et al. 1991), iberiotoxin (IbTx; Johnson et al. 1992), noxiustoxin (NTx; Dauplais et al. 1995), PO5-NH₂ (Meunier et al. 1993), kaliotoxin (KTx; Fernandez et al. 1994), margatoxin (MgTx; Johnson et al. 1994), and tityustoxin K- α (TsTx-K α ; Ellis et al. 2001). Although the overall fold of these α -KTx toxins is very similar, there are subtle variations among them in amino acid sequence, the size of the β -sheet, the type of β -turn, or the type of α -helix (i.e., α -helix versus 3_{10} -helix). These differences in toxin structure affect the placement of side-chain moieties. Thus, the selectivity that various scorpion toxins have for the outer vestibule of different K⁺ channels is typically quite distinct. Previously, Doyle et al. (1998) applied X-ray crystallographic methods to determine the three-dimensional structure of the KcsA bacterial K⁺ channel, which may serve as a good model for understanding the binding site of scorpion toxin on Kv-type channels.

Recently, a new K⁺-channel blocker was identified from the scorpion venom of *Tityus cambridgei* (Tc1; Batista et al. 2000). Tc1 contains 23 amino acids linked with three disulfide bridges and is the smallest K⁺-channel blocker toxin from scorpion venoms. All previously known K⁺-channel blockers from scorpion venoms are longer than 30 amino acid residues and are classified into 12 subfamilies as described above. Tc1 is classified as the first member of the

new subfamily 13. In K⁺-channel blocking activity, Tc1 recognizes the *Shaker* B K⁺ channels with a dissociation constant (K_d) of 65 nM and competes with NTx for binding to the synaptosomal membranes, with an inhibitory concentration 50% (IC₅₀) value in the order of 200 nM (Batista et al. 2000). Tc1 is a highly basic peptide because it contains seven positively charged residues with a pI value of 9.50. The sequence alignment of Tc1 with eight other K⁺-channel blockers from scorpion toxins is shown in Figure 1. We found that six cysteine residues (Cys², Cys⁵, Cys⁹, Cys¹⁵, Cys²⁰, and Cys²²), Gly¹³, and Lys¹⁴ (Tc1 numbering) are conserved, and the C-terminal regions are highly similar among these toxins. In addition, the sequence of Tc1 shows some unique properties. For example, Tc1 possesses Arg at position 19, whereas the corresponding residue in the other toxins is Lys. At position 16, Tc1 has Ile, whereas the other toxins, with the exception of the PO5 peptide, have Met at the corresponding position. Furthermore, Tc1 contains dense positively charged residues at residues 5–10. Unlike other scorpion toxins, Tc1 does not contain either negatively charged residues or proline. These properties make Tc1 an excellent candidate for three-dimensional structure determination and site-directed mutagenesis and for gaining clearer understanding of K⁺ channels.

In this study, synthetic Tc1 was made by conventional solid-phase peptide synthesis and folded into its active conformation. We checked the channel-blocking activity of the synthesized Tc1 and found that both synthetic and native Tc1 possess similar blocking activity against the *Shaker* K⁺ channel. Next, we applied circular dichroism (CD) and NMR techniques to solve the solution structure of Tc1. To further understand the various structure-function relationships among the K⁺-channel blockers from scorpion venoms, we compared the three-dimensional structure of Tc1 and those of other structurally and functionally related scorpion toxins, ChTx and NTx. We concluded that the C-terminal structure is the most important region for the blocking

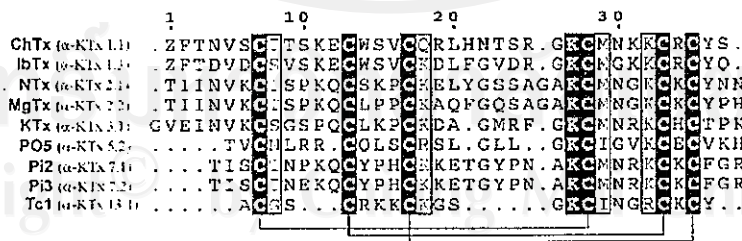


Fig. 1. Sequence alignment of Tc1 with eight other K⁺-channel blockers was generated using the CLUSTAL-W (Thompson et al. 1994) and ESPript (Gouet et al. 1999) programs. Three-dimensional solution structures for six of them have been determined: They are ChTx (Bontems et al. 1991), IbTx (Johnson and Sugg 1992), NTx (Dauplais et al. 1995), MgTx (Johnson et al. 1994), KTx (Fernandez et al. 1994), and PO5 (Meunier et al. 1993). Residues that are identical are boxed in red; those that are highly conserved are shown in red. The sequence number is based on the sequence of ChTx (top), and the α -KTx name of each peptide (in parentheses) is shown. The three internal disulfide-bridges are indicated with green brackets (bottom).

activity of Kv-type channels for scorpion K⁺-channel blockers. In addition, we also asserted that some of the residues in the larger scorpion K⁺-channel blockers, which contain 31 to 40 amino acids, are clearly not involved in K⁺-channel blocking activity.

Results

Synthetic Tc1 is as potent as the natural scorpion toxin Tc1

We first examined the effect of the synthetic Tc1 on *Shaker* GH4 K⁺ channels expressed in *Xenopus* oocytes. Figure 2 showed that 10 μ M of synthetic Tc1 completely blocked outward currents (Fig. 2A,B). The inhibition was reversible on washout (Fig. 2C), but the block was not voltage dependent (Fig. 2D). Figure 2E shows the dose-response curve for the block of the peak current by synthetic Tc1 at +50 mV. The peak current amplitude in various concentrations of

synthetic Tc1 was normalized to that of the control solution and expressed as fractional I. K_d for the synthetic Tc1 block was 65 nM, which is the same as the previously reported value for the scorpion toxin Tc1 block of *Shaker* B K⁺ channels transfected in SP9 cells (Batista et al. 2000). These results indicate that the functional property of the synthetic Tc1 is the same as the natural scorpion toxin Tc1.

Synthetic Tc1 is a stable K⁺-channel blocker

We performed CD experiments of Tc1 at different pH values (3.5 to 7.0) and at various temperatures (0°C to 95°C). The CD spectra were very alike at different pH values, indicating that Tc1 possesses similar conformations at pH ranges of 3.5 to 7.0. The CD spectra at different temperatures (Fig. 3) displayed a blue-shift of the negative band when the temperature was increased (212 nm at 10°C to 208 nm at 95°C), with an isodichroic point at 207 nm. This indicates that there is a conformational equilibrium for Tc1 at various temperatures. The majority of the secondary

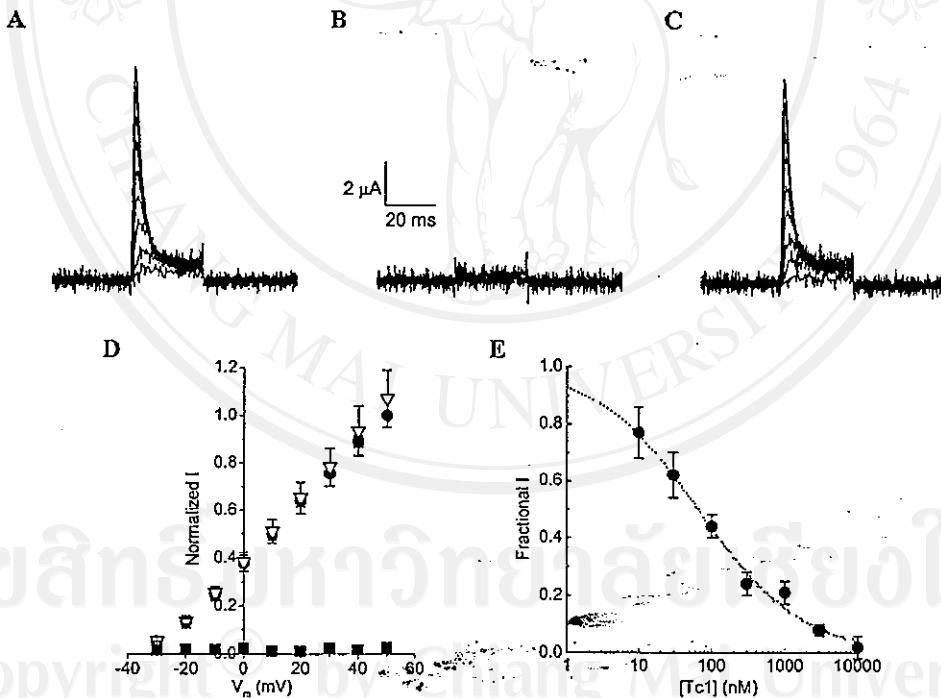


Fig. 2. Block of *Shaker* GH4 K⁺ channels by synthetic Tc1. (A) Whole-cell currents through *Shaker* GH4 K⁺ channels were recorded in a control solution. (B) Currents were completely eliminated after the addition of 10 μ M synthetic Tc1 to the control solution. (C) Currents completely recovered from synthetic Tc1 block after washout in the control solution. (D) Normalized peak current-voltage relationships ($n = 4$) obtained in control (circles), 10 μ M synthetic Tc1 (squares), and washout (triangles). All peak currents were normalized to that recorded at +50 mV in the control solution. (E) Dose-response curves for synthetic Tc1 block of the peak *Shaker* GH4 current at +50 mV. Dotted line is the best fit of the data ($n = 3$ to 4) to the Hill equation: $I/I_0 = 1/(1 + [Tc1]/K_d)^h$. $K_d = 65$ nM is the apparent dissociation constant, and $h = 0.6$ is the Hill coefficient.

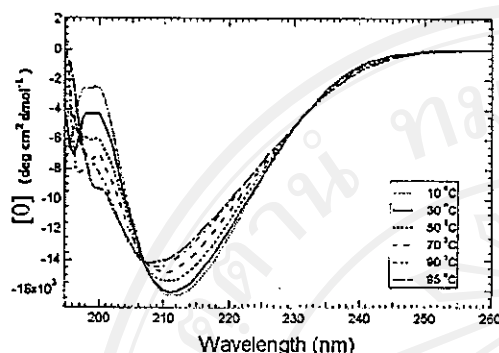


Fig. 3. CD spectra of 20 μ M Tc1 in 20 mM phosphate buffer at pH 3.0 are shown as a function of temperature. For the sake of clarity, only some of the spectra are shown.

structure remained intact even at 95°C, revealing that Tc1 is a thermostable peptide. The contents of the secondary structures of Tc1 estimated using CONTIN-LL, SELCON3, and CDSSTR (Sreerama and Woody 2000) are listed in Table 1.

Resonance assignments and secondary structure determination of Tc1

With thermostability and well-dispersed NMR data, Tc1 is an excellent compound for NMR structural studies. Based on the NMR data acquired at different pH values and temperatures, the resonance assignments were accomplished using the standard procedures (Wüthrich 1986). Spin systems were identified based on scalar-correlated spectroscopy (COSY) and total correlation spectroscopy (TOCSY) experiments, and sequential connectivities were obtained from nuclear Overhauser enhancement (NOE) spectroscopy experiments. To obtain as many NOEs as possible, we tested many conditions and finally chose pH 3.0 and pH 7.3 at 275 K for performing our NMR experiments. The representative regions of a NOE spectroscopy spectrum, with partial annotations, are shown in Figure 4. Interestingly, the amide proton of Cys⁵ was not observed, presumably because of the fast exchange with water. The amide proton of Arg⁶ showed a sharper line width compared with that of the other amide protons. These observations indicate that the conformation in the Cys⁵–Arg⁶ dipeptide is flexible, and the amide protons of both Cys⁵ and Arg⁶ are highly exposed to the solvent. At pH 7.3, the amide protons in the N-terminal Cys²–Cys³ were not detected, suggesting that the N-terminal segment is more flexible than the C terminus. The observed NOE patterns at pH 7.3 were very similar to those at pH 3.0, further supporting the similarity of the structure at both acidic and neutral pH values. Figure 5A shows the summary of the NMR parameters for Tc1 at pH 3.0. The

C^αH chemical shift index (CSI; Wishart et al. 1992) indicates that Cys²–Lys¹⁰ forms an α -helical structure and that Gly¹³–Ile¹⁶ and Arg¹⁹–Tyr²³ show β -strand conformations. Based on the α -helical NOEs, we identified an α -helix at the N-terminal Ser⁴–Lys¹⁰, which is in good agreement with CSI results. In Gly¹¹, we did not observe the α -helical NOE of $d_{\alpha N}(8, 11)$, although a medium range NOE of $d_{\alpha N}(7, 11)$ was detected. This indicated that Gly¹¹ likely formed a turn structure. According to the observed long-range NOEs between the two β -strands, among which $d_{\alpha N}(15, 21)$ and $d_{\alpha\alpha}(15, 20)$ could not be accurately assigned because of chemical shift degeneracy at C^αH of Cys¹⁵ and Cys²⁰, and the deduced hydrogen bonds that were consistent with the β -sheet structure (Fig. 5B), we found that the two β -strands actually formed a double-stranded antiparallel β -sheet, with a β -turn conformation at residues Asn¹⁷–Gly¹⁸. The observation of medium intensity of the $d_{\alpha N}(17, 19)$ NOE, along with backbone ϕ , ψ angles of residues Asn¹⁷ and Gly¹⁸, calculated based on the derived NMR structures described in the next paragraph, revealed that the Ile¹⁶–Arg¹⁹ segment is a type I' β -turn. In addition, based on the $d_{\beta\beta}(i, j)$ NOEs between the C^βH protons of the two cysteines forming a disulfide bridge, the connections of three disulfide bridges of the synthetic Tc1 were identified. We observed 17 amide protons possessing medium- or slow- exchange rates at pH 3.0, as shown in Figure 5A. In contrast, only six amide protons at the C terminus (Lys¹⁴, Ile¹⁶, Gly¹⁸, Arg¹⁹, Lys²¹, and Tyr²³) showed medium- and slow-exchange rates at pH 7.3. The exchange rate study at pH 3.0 and pH 7.3 proved that the C-terminal β -sheet possesses higher stability than the N-terminal α -helix.

Three-dimensional solution structure of Tc1

A set of 200 restraints was applied for simulated annealing and energy minimization calculations using the program X-PLOR. Fifteen structures were chosen to represent the ensemble of NMR structures on the basis of the lowest target function and minimal distance and torsional angle restraint violations in the final stage. All of these structures were consistent with both experimental data and standard covalent geometry, and they displayed no violations >0.5 Å

Table 1. Secondary structure contents of Tc1 estimated from CD spectra acquired at pH 3.0 using three different methods^a

Methods	Temp.	α_R	α_D	β_R	β_D	T	U
CONTINLL	25°C	0.028	0.077	0.164	0.101	0.243	0.387
	95°C	0.018	0.060	0.128	0.095	0.255	0.444
SELCON3	25°C	0.039	0.086	0.176	0.107	0.234	0.358
	95°C	0.030	0.079	0.182	0.106	0.229	0.374
CDSSTR	25°C	0.013	0.082	0.209	0.111	0.242	0.343
	95°C	0.002	0.083	0.200	0.105	0.244	0.366

^a (α_R) Regular α -helix; (α_D) distorted α -helix; (β_R) regular β -strand; (β_D) distorted β -strand; (T) turns; (U) unordered.

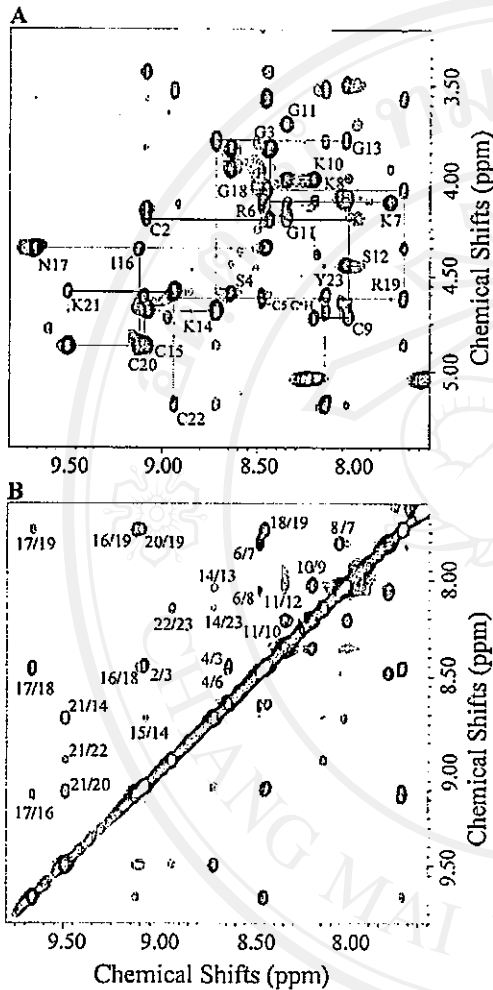


Fig. 4. (A) The fingerprint region of a NOE spectroscopy spectrum of Tc1 acquired at 275 K and pH 3.0, with a mixing time of 400 ms. Resonance assignments are indicated with one-letter amino acid codes and residue numbers. (B) The NH/NH region of the same experiment in A. The assignment of each cross-peak is labeled with residue numbers.

for distance restraints. The structure with the lowest final total energy and root mean square deviation (RMSD) of distance restraints was defined as the best structure. Superposition of each structure with the best structure yielded average RMSD of 0.26 ± 0.05 Å for the backbone atoms and 1.40 ± 0.23 Å for heavy atoms in residues 2–23, respectively (Fig. 6A). The structural statistics on the final set of structures are given in Table 2. Analysis of the ensemble of 15 structures using PROCHECK-NMR revealed that 98.8% of the residues lie in the most favored and allowed regions

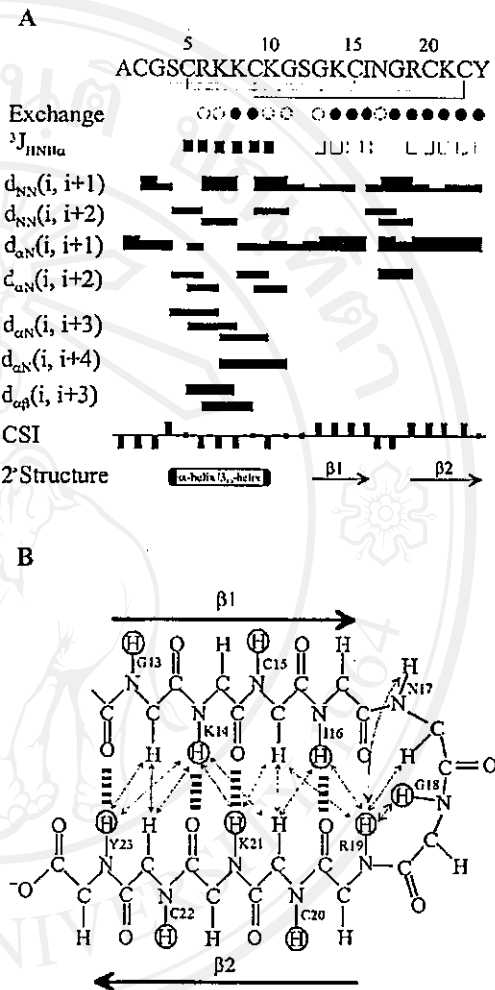


Fig. 5. (A) Summary of the amide proton exchange rates, $^3J_{\text{HNH}\alpha}$ -coupling constants, NOE connectivities, $^{\text{C}}\text{H}$ chemical shift index, and the derived secondary structures. Medium-exchange (<3.5 h; open circles) and slow-exchange (>24 h; filled circles) amide protons. $^3J_{\text{HNH}\alpha}$ coupling constants are <6 Hz (filled squares) and >8 Hz (open squares). Bar thickness indicates the intensity of NOE connectivity, with thicker bars representing stronger NOEs. Negative bars in the chemical shift index indicate upfield shifts of >0.1 ppm of the $^{\text{C}}\text{H}$ proton compared with the expected random-coil $^{\text{C}}\text{H}$ proton chemical shift. Positive bars indicate downfield shifts of >0.1 ppm of the $^{\text{C}}\text{H}$ proton compared with the expected random-coil $^{\text{C}}\text{H}$ value. The derived secondary structures based on NMR parameters as described above are shown (bottom). (B) Definition of the β -sheet structure of Tc1 is shown based on the NOEs and amide proton exchange rate. Cross-over NOEs between β -strands are shown in double arrows. Ambiguous cross-over NOEs, because of resonance overlap, are indicated in double arrows with a dashed line. Dashed lines between backbone amide protons and backbone carbonyl oxygens indicate hydrogen bonds consistent with slow-exchanging H^{D} observed in D_2O . The amide protons with slow exchange rates are circled.

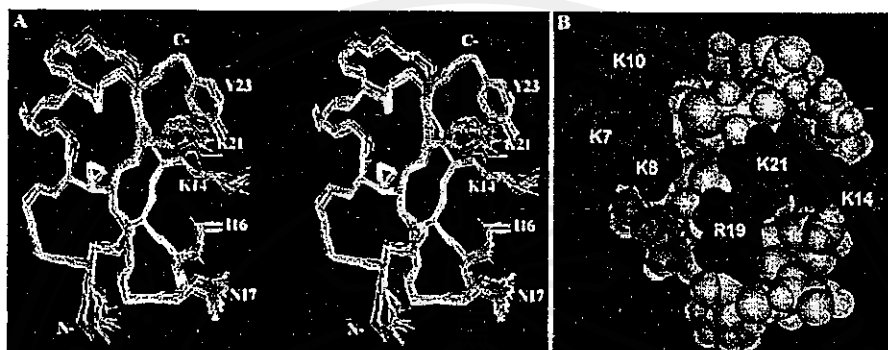


Fig. 6. (A) Stereo view of the superimposition of the heavy atoms of 15 NMR structures obtained from simulated annealing and energy minimization calculations. The structures are best fitted to residues 2–23. Side-chains of the five residues (Lys¹⁴, Ile¹⁶, Asn¹⁷, Lys²¹, and Tyr²³), which correspond to the residues for the recognition of a voltage-dependent K⁺ channel (Shaker B) in ChTx, are shown and labeled. (B) Space-filling model of the best structure of Te1. The structure is colored according to the charge of the amino acid residues, with positive residues in blue and neutral residues in gray. Two positively charged regions are clearly shown, and the charged residues are labeled in the structure.

of the Ramachandran ϕ , ψ dihedral-angle plot (plot not shown). The distribution of ϕ and ψ backbone dihedral angles showed that only three backbone dihedral angles (ϕ of Cys², ψ of Gly¹¹, and ϕ of Ser¹²) displayed large deviations, revealing that the backbone conformation is rigid except for the N-terminal Cys² and the loop region of Gly¹¹ and Ser¹². Interestingly, the β -turn of the Asn¹⁷–Gly¹⁸ dipeptide also contains very stable ϕ and ψ dihedral angles. Further, the dihedral angles of three disulfide bonds were found to be rigid, with average angles of -146.10 ± 3.92 (Cys²–Cys¹⁵), -107.71 ± 2.27 (Cys⁵–Cys²⁰), and 115.47 ± 4.18 (Cys⁹–Cys²²). In contrast, the side-chain χ_1 dihedral angles in arginines and lysines, with the exception of Lys¹⁴, all showed very large deviations. All hydrogen bonds in these 15 structures were located in the N-terminal α -helix, β -sheet, and β -turn regions. In the N-terminal α -helix, we consistently observed a hydrogen bond of Lys⁷ CO/Lys¹⁰ NH, indicating that Lys⁷–Lys¹⁰ forms a 3_{10} -helix. In the β -turn region (Ile¹⁶–Arg¹⁹), as expected, the hydrogen bond of Ile¹⁶ CO/Arg¹⁹ NH was detected in all the NMR structures. Te1 is a basic protein with two arginines and five lysine positively charged residues. At neutral pH, it carries an overall positive charge, and the distribution of the charges is clearly distributed into two regions, as shown in the space-filling structure of Te1 (Fig. 6B).

Discussion

Our studies on the effects of synthetic Te1 on Shaker GH4 K⁺ channels indicated that its functional property is the same as the natural scorpion toxin Te1. We then used CD and NMR techniques to perform our structural study of the

Table 2. Structural statistics on the final set of 15 simulated annealing structures of Te1

A. Constraints used	
Distance restraints	
Intraresidue ($li - ji = 0$)	17
Sequential ($li - ji = 1$)	67
Medium range ($li - ji = 2$), ($li - ji = 3$)	34
Long range ($li - ji \geq 4$)	45
Total distance restraints	163
Hydrogen bonds	8×2
Dihedral angles	21
B. Statistics for the final X-PLOR structures	
Number of structures in the final set	15
X-PLOR energy (kcal/mole)	
E_{NOE}	5.40 ± 0.43
E_{con}	2.02 ± 0.24
$E_{\text{bond}} + E_{\text{angle}} + E_{\text{improper}}$	36.67 ± 1.20
E_{vdw}	34.39 ± 0.86
NOE violations	
Number > 0.5 Å	none
Rms deviation (Å)	0.032
Deviation from idealized covalent geometry	
Angle (°)	0.52 ± 0.01
Improper (°)	0.42 ± 0.02
Bonds (Å)	0.005
Mean global rms deviation (Å)	
Backbone (N, C $^{\alpha}$, C $^{\beta}$)	
Residues (2–23)	0.26 ± 0.05
Heavy atoms	
Residues (2–23)	1.40 ± 0.23
Ramachandran data (%)	
Residues in most favored regions	72.1
Residues in allowed regions	26.7
Residues in generously allowed regions	1.2
Residues in disallowed regions	0.0

synthetic Tc1. CD spectra at different temperatures and pH values showed that Tc1 is a thermostable peptide with a conformation that is independent of pH values in the range of 3.0 to 7.0. The three-dimensional NMR solution structure of Tc1 showed that it is comprised of an α -helix and a 3_{10} -helix at N-terminal Gly⁴-Lys¹⁰, a double-stranded antiparallel β -sheet at Gly¹³-Ile¹⁶ and Arg¹⁹-Tyr²³, with a type I' β -turn at residues Asn¹⁷-Gly¹⁸. Because the NMR data obtained at pH 3.0 and 275 K were well resolved and showed many medium- and long-range NOEs, high resolutions of Tc1 structures were generated. We found that the overall structures of Tc1 and other α -KTx toxins are similar, although Tc1 only possesses 23 amino acids compared with >30 for the other scorpion toxins.

To gain further insight into the structural and functional relationships among the K⁺-channel blockers from scorpion venoms, we proceeded to a detailed comparison of the three-dimensional structure of Tc1 with two structurally and functionally related scorpion toxins, ChTx (37 amino acids) and NTx (39 amino acids). ChTx is the first member of subfamily I of α -KTx and shows a much higher affinity for the Ca²⁺-activated K⁺ channels (BK) than for Kv1.3. In contrast, NTx is the first K⁺-channel blocker isolated from scorpion venoms and displays a strong binding affinity for Kv1.3, whereas it exerts a weaker affinity for BK. Tc1 also has a higher binding affinity for the *Shaker* B channel than for BK, similar to NTx. In the secondary structure motifs, we found that the N-terminal α -helix, the two C-terminal β -strands, and the β -turn are all located in similar regions based on the sequence alignment of these toxins. However, some variations were observed in the type or length of the secondary elements. For example, Tc1 has a shorter helical conformation, and this helix begins with a regular α -helix and ends with a 3_{10} -helix, whereas the helix in NTx begins with a 3_{10} -helix and ends with a regular α -helix. Also, because of the presence of a Pro residue in the α -helical region, the α -helix in NTx displays a high degree of curvature. The bending of the α -helix in both Tc1 and ChTx, however, is weak because of the lack of a proline residue in the sequence. Tc1 and NTx have the same type I' β -turn at Asn¹⁷-Gly¹⁸ and Asn³¹-Gly³², respectively, whereas ChTx possesses a type I β -turn at Asn³⁰-Lys³¹. NTx not only contains an extra N-terminal β -strand but also possess longer C-terminal β -strands. Thus, there is a remarkable plasticity within the α/β -scaffold for the α -KTx toxins.

The specificity of scorpion toxins for the various potassium channels has been investigated through the generation of mutants of both receptors and toxins. Mutational analysis of ChTx showed that eight residues (Ser¹⁰, Trp¹⁴, Arg²⁵, Lys²⁷, Met²⁹, Asn³⁰, Arg³⁴, and Tyr³⁶) are important for the binding of ChTx to BK (Stampe et al. 1994). Five of these eight residues (Lys²⁷, Met²⁹, Asn³⁰, Arg³⁴, and Tyr³⁶) were shown to be critical for the recognition of a voltage-dependent K⁺ channel (*Shaker* B) in ChTx (Goldstein et al. 1994).

Among these residues, Lys²⁷ is the most important because a mutation of this lysine to arginine destabilizes the toxin by >1000-fold (Miller 1995). The inhibition of the channel permeation is the result of a physical occlusion of the pore-forming region of the channel. Thus, the Lys²⁷ of ChTx is suspected to directly plug into the pore.

The characteristics of five corresponding residues for the recognition of the *Shaker* B channel in Tc1 (Lys¹⁴, Ile¹⁶, Asn¹⁷, Lys²¹, and Tyr²³) are similar to those in ChTx. However, the properties of other three residues (Ser¹⁰, Trp¹⁴, and Arg²⁵), which are also important for the binding of ChTx to BK-type channels, were found to be very different in Tc1. The corresponding residues in Tc1 for the first two are Ser⁴ and Arg⁶, respectively, and there is no residue occupied for the third. Thus, the different property in these residues offers a possible explanation for the weak affinity of Tc1 to BK-type channels. For the recognition of the *Shaker* B channel in Tc1, we found that the side-chains of these residues were all exposed to the solvent on the same side (see Fig. 6A). Interestingly, Lys¹⁴, which corresponds to Lys²⁷ in ChTx, showed a rigid side-chain conformation and highly protruded into the solvent. Thus, we suggest that Lys¹⁴ in Tc1 is the key residue to have electronic interaction with the negative charge in the pore region of the K⁺ channel.

In addition, IbTx was found to be inactive against the Kv1.3 channel. A sequence comparison between ChTx and IbTx indicates that Asn³⁰ (ChTx numbering) is replaced with Gly in IbTx. Therefore, Asn³⁰ appears to be important for the two types of voltage-dependent channels; in fact, this residue can be found in all the short-chain scorpion toxins that bind Kv1.3 (ChTx, NTx, MgTx, KTx, and Tc1 in Fig. 1). Two scorpion toxins in subfamily 7, Pi2 and Pi3, have only one amino acid difference at position 7 (a proline for a glutamic acid) in their sequence. However, Pi2 binds the *Shaker* B K⁺ channels with a K_d of 8.2 nM, but Pi3 has a much lower affinity of 140 nM (Gomez-Lagunas et al. 1996). The difference in binding affinity supports that the N-terminal residues are part of the domain that recognize *Shaker* B K⁺ channels. Interestingly, there is no residue occupied at the corresponding position in Tc1, which has a K_d of 65 nM. Therefore, it is certain that the negative charge at this position disrupts the inhibition of the *Shaker* B K⁺ channel.

The surface structures of Tc1, NTx, and ChTx (plot not shown) all indicated that there is a positively charged region at the C terminus and that this region plays an important role for blocking activity. At the N terminus, Tc1 contains a denser positively charged region composed by Arg⁶, Lys⁷, Lys⁸, and Lys¹⁰ (Fig. 6B) compared with NTx and ChTx. At present, we do not know whether this region interacts with the K⁺-channel or whether it plays an important role for activity. We are currently performing mutational studies on Tc1 to further understand its structural-functional relationships.

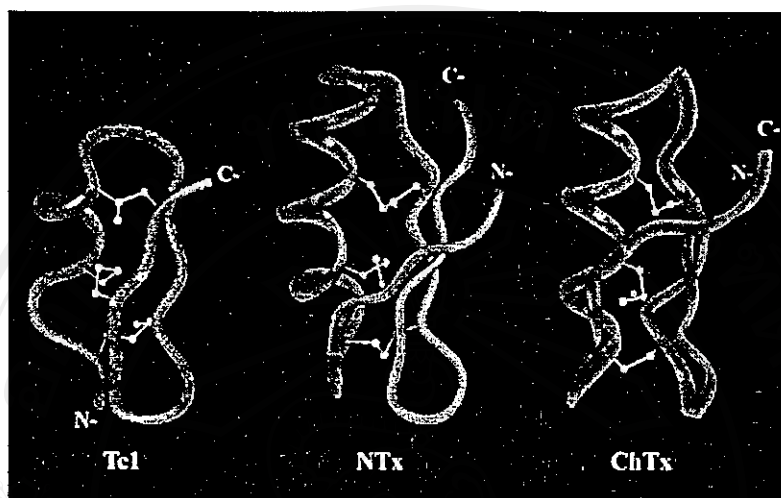


Fig. 7. Comparison of the ribbon structure of TcI and two structurally and functionally related scorpion toxins, NTx and ChTx. Three disulfide bridges are shown as balls and sticks. NTx and ChTx coordinates were obtained from the Protein Data Bank with accession Nos. 1SXM and 2CRD, respectively.

In addition, Figure 7 shows the comparison of the ribbon structures of TcI, NTx, and ChTx. Superposition of backbone atoms (N, C^α, and C^β) between Gly¹³ and Tyr²³ of TcI and between Ala²⁷ and Tyr³⁷ of NTx gave a RMSD of 0.76 Å. However, the RMSD became 0.96 Å between Gly¹³–Tyr²³ of TcI and Gly²⁶–Tyr³⁶ of ChTx. Thus, TcI is much like NTx, especially at the C-terminal β-sheet and β-turn. Because both TcI and NTx contain higher activity for the *Shaker* B channel, we concluded that the C-terminal structure is the most important region for controlling the blocking activity of the Kv-type for scorpion K⁺-channel blockers. Furthermore, based on the structural data and sequence alignment between TcI and NTx, we suggest that for NTx the N-terminal region—including the first β-strand (Thr¹–Val⁵), some residues in the α-helix (Lys¹¹, Gln¹², Glu¹⁹, and Leu²⁰), some residues in the loop region (Tyr²¹, Ser²³, and Ala²⁵), and some residues in the C-terminal region (Ala²⁷, Asn³⁸, and Asn³⁹)—might not be required for channel-blocking activity. Therefore, we are also in the process of studying the structural and functional relationships of a 24-residue peptide that involves the deletion of the above 15 residues from NTx.

Materials and methods

Chemical synthesis of TcI

TcI was synthesized by solid-phase peptide synthesis using a 433A peptide synthesizer (ABI). Starting with 0.25 mmole (0.238 g) of HMP (*p*-hydroxymethyl phenoxymethyl polystyrene) resin

(1.00 mmole/g), the synthesis was performed using a stepwise Fast Moe protocol. The amino acids were introduced using the manufacturer's prepacked cartridges (1 mmole each). After synthesis, 0.386 g peptide resin was placed in a round-bottom flask containing a micro stirringbar. The cool mixture containing 0.75 g crystalline phenol, 0.25 mL EDT, 0.5 mL thioanisole, 0.5 mL water, and 10 mL TFA was put into the flask and stirred for 2 to 3 h at room temperature. The peptide was further lyophilized. Then the peptide was rinsed with 200 mL cold ether and filtered. The filtered peptide was immediately transferred to 2.9 L of diluted acetic acid solution (5% AcOH in water) and stirred for several minutes. After filtration to remove the resin, the pH of the solution was adjusted to pH 8.6 with ammonium hydroxide. Analytical high performance liquid chromatography (HPLC) was used to monitor the progress of oxidation. The peptide was purified by HPLC using a C₁₈ column (10-μm particle size, 250 × 4.6 mm) with a gradient (5% to 95% buffer B in 30 min) using buffer A (0.1% TFA in water) and buffer B (0.1% TFA in acetonitrile) at a flow rate of 1 mL/min and monitored by absorbance at 214 nm. Mass spectra were determined using a Finnigan LCQ Mass Spectrometer with an electrospray ion source. Unless otherwise stated, all reagents and solvents were obtained commercially as reagent grade and used without further purification.

Whole-cell current recording

Purification of *Shaker* GH4 K⁺ channel cDNA and in vitro T7 transcription reactions (mMessage mMachine, Ambion) were performed as previously described (Shieh et al. 1998). *Xenopus* oocytes were isolated by partial ovariectomy from frogs anaesthetized with 0.1% tricaine (3-aminobenzoic acid ethyl ester). Oocytes were pressure injected with RNA 24 h after defolliculation and used 1 to 3 d after RNA injection. Oocytes were maintained at 18°C in Barth's solution containing (in mM) NaCl (88), KCl (1),

NaHCO₃ (2.4), Ca(NO₃)₂ (0.3), CaCl₂ (0.41), MgSO₄ (0.82), HEPES (15), and gentamicin (20 µg/mL) at pH 7.6.

The block of whole-cell *Shaker* GH4 K⁺ channels by synthetic Tc1 was examined at room temperature (21°C to 24°C) using a two-electrode voltage-clamp amplifier (Ca-1 clamp; Dagan). Oocytes were bathed in a control solution containing (in mM) KCl (3), NMG (100), CaCl₂ (1), and HEPES (5) at pH 7.4. Both the voltage-sensing and current-injecting electrodes were filled with 3 M KCl (resistance, 0.3 to 1 MΩ). Voltage steps were applied from a holding potential of -90 mV to various test voltages (30 msec) ranging from -30 to +50 mV in 10-mV increments. The command V_m and data acquisition functions were processed using a Pentium computer, a DigiData board, and pClamp6 software (Axon Instruments). The frequency of stimulation was 0.5 Hz, and the sampling rate was 10 kHz. Data were filtered at 2 kHz by an eight-pole low-pass filter (Frequency Devices). Leak current and capacity transients were corrected with a P/4 voltage protocol.

CD experiments

CD experiments were performed using an Aviv CD 202 spectrometer (AVIV) calibrated with (+)-10-camphorsulfonic acid (CSA) at 298 K. In general, a 2-mm pathlength cuvette with 20 µM Tc1 peptide in 20 mM phosphate was used for CD experiments and all the protein solutions were made up to 1 mL. The CD spectra of Tc1 at different temperatures and pH values were recorded. Each piece of the CD data was obtained from an average of three scans with 1-nm bandwidth. The spectra were recorded from 180 nm to 260 nm, at a scanning rate of 38 nm/min with a wavelength step of 0.5 nm and time constant of 100 msec. After background subtraction and smoothing, all the CD data were converted from CD signal (millidegree) into mean residue ellipticity (deg cm²/dmole⁻¹). The secondary structure content was estimated from the CD spectra according to the methods of CONTIN, SELCON, and CDSSTR (Sreerama and Woody 2000).

NMR experiments

The NMR measurements were performed on a Bruker AMX-500 or AVANCE-600 spectrometer. Samples for NMR experiments contained 0.35 mL of 2 mM Tc1 in 50 mM phosphate buffer at pH 3.0 and 7.3. pH values were measured with a DO microelectronic pH-vision model PHB-9901 pH meter equipped with a 4-mm electrode. All reported pH values were direct readings from the pH meter without correction for isotope effect. To monitor the exchange rates of labile protons, the concentrated sample in water was lyophilized only once and re-dissolved in D₂O (99.99% D), and NMR spectra were acquired immediately and thereafter at appropriate time intervals. All chemical shifts were externally referenced to the methyl resonance of 2,2-dimethyl-2-silapentane-5-sulfonate (DSS; 0 ppm). Double-quantum-filtered (DQF)-COSY (Rance et al. 1983), TOCSY (Bax and Davis 1985), and NOE spectroscopy (Kumar et al. 1980) were collected with 512 *t_r* increments with 2K complex data points. All spectra were recorded in time-proportioned phase sensitive (TPPI) mode (Marion and Wüthrich 1983). Low-temperature studies used a temperature-controlled stream of cooled air using a Bruker BCU refrigeration unit and a B-VT 2000 control unit. Water suppression was achieved by 1.4-sec presaturation at the water frequency, or by the gradient method (Piotto et al. 1992). All spectra were collected with 6024.1- and 7788.16-Hz spectral widths for AMX-500 and Avance-600 respectively.

The data were transferred to an SGI O₂ workstation, 200-MHz R500SC (Silicon Graphics), for all processing and further analysis using the Bruker XWINNMR and AURELIA software packages. All data sets acquired were zero-filled to equal points in both dimensions before further processing. A 60°-shifted skewed sine bell window function was applied in all NOE spectroscopy and TOCSY spectra, and a 20°- or 30°-shifted skewed sine bell function was used for all COSY spectra. To help with resolving spectral overlap, data were collected at different temperatures.

Torsional angle restraints and stereospecific assignment

The ³J_{NHα}-coupling constants were estimated from the residual intensity of the antiphase cross-peak in DQF-COSY spectra recorded in water. ϕ -Torsional restraints of -130 ± 30° for ³J_{NHα}-coupling constants >8 Hz, and -60 ± 30° for ³J_{NHα}-coupling constants <6 Hz, were used for structure calculation. We obtained a total of 15 ϕ -torsional restraints located in the α -helix and β -sheet regions. The ϕ -torsional restraints were used for structure generations starting from the early stage when NOE correlations were also consistent. The stereospecific assignments were derived using the method of Hyberts et al. (1987). The ³J_{αβ}- and ³J_{αβ'}-coupling constants were estimated as either large or small based on (1) the intensities of the cross-peaks observed in a DQF-COSY spectrum in D₂O and a TOCSY spectrum recorded in short mixing time, and (2) the relative intensities of the intrareidue C^αH-C^βH and NH-C^βH NOE cross-peaks. The stereospecific assignment of β -methylene also allowed us to assign the χ_1 -torsional angle restraints to 60 ± 30°, 180 ± 30°, or -60 ± 30°. To ensure the accuracy of stereospecific assignments, we obtained 6 prochiral assignments (Cys², Cys⁹, Asn¹⁷, Cys²⁰, Cys²², and Tyr²³) with certainty. We found that the stereospecific assignments agreed well with our generated structures in the early stage. Thus, in the later stage of structure generation, we also added χ_1 and prochiral assignments as restraints in the structure calculation.

Hydrogen bond and disulfide restraints

The amide-proton exchange rates were identified from residual amide proton signals observed in several TOCSY spectra recorded at 275 K at pH 3.0 and 7.3, respectively. The first spectrum was recorded within 3.5 h after the lyophilized sample was redissolved in D₂O. The amide proton exchange rates were categorized into three classes: fast-, medium-, and slow-exchange rates. Hydrogen-bond formation or solvent exclusion from the amide protons was assumed to account for the slow- and medium-exchange-rate amide protons. For better convergence, a number of hydrogen bonds involved in the secondary structure were included as distance restraints in the final stage of structure generation, that is, an O-N distance of between 2.5 and 3.3 Å and O-HN distances of 1.8 and 2.5 Å between NH protons and the backbone carbonyl oxygen atoms were assigned to the slow- and medium-exchanging protons, respectively, in the latter stage of structure determination. In the final stage of structure calculation, the hydrogen bonds between NH_i and OC_j in the β -sheet structures were included as restraints only if the β -sheet interstrand NH_i/NH_j, NH_i/C^αH_{j+1}, and C^αH_{i-1}/C^αH_j NOE cross-peaks were observed. The disulfide bonds used in the structure calculation were Cys² to Cys¹⁵, Cys⁵ to Cys²⁰, and Cys⁹ to Cys²². Covalent bonds between the sulfur atoms of disulfide bridges were modeled by restraining the distances between the two sulfur atoms to 1.80 to 2.30 Å.

Tertiary structure calculations

Distance restraints of Tc1 were derived primarily from the 200- and/or 400-msec NOESY spectra recorded in aqueous solution at 275 K and pH 3.0. Comparison was made to the 100-msec NOE spectroscopy spectrum to assess possible contributions of the NOEs from spin diffusion. Peak intensities were classified as large, medium, small, and very small, corresponding to upper bound interproton distance restraints of 2.5, 3.5, 4.5, and 6.0 Å, respectively. An additional correction of 1.0 Å was added for methylene and methyl groups. The structure determination was performed using 163 distance restraints, of which 17 were intra-residue, 67 were sequential, 79 were medium- and long-range interproton distances, 16 were hydrogen bonds, 15 were ϕ -torsional angles, and 6 were χ_1 -torsion angles. All minimization and dynamical simulated annealing calculations were performed with the program X-PLOR 98 (Brünger 1998) on a SGI O₃ workstation. The INSIGHT II (Molecular Simulation Inc.), MOLMOL (Koradi et al. 1996), and GRASP (Nicholls et al. 1991) programs were used to visually observe sets of structures and to calculate and make the electrostatic surface potential of the final three-dimensional models. The distributions of the backbone dihedral angles of the final converged structures were evaluated by the representation of the Ramachandran dihedral pattern, indicating the deviations from the sterically allowed (ϕ , ψ) angle limits using PROCHECK-NMR (Laskowski et al. 1996) and MOLMOL.

Data bank accession numbers

The chemical shifts of Tc1 at pH 3.0 and 275 K have been deposited to BioMagResBank (BMRB) under accession No. 5082. The atomic coordinates of the 15 energy-minimized conformers used to represent the solution structure of Tc1 have been deposited in the Brookhaven data bank, together with the complete input of conformational restraints used for the structure calculation under accession No. 1JLZ.

Acknowledgments

We thank N.Y. Su for assistance with NMR experiments and C.H. Hsu for helpful suggestions on this work. We also thank Academia Sinica and the National Science Council, Taipei, Taiwan, R.O.C. for support of this work.

The publication costs of this article were defrayed in part by payment of page charges. This article must therefore be hereby marked "advertisement" in accordance with 18 USC section 1734 solely to indicate this fact.

References

- Batista, C.V.F., Gomez-Lagunas, F., Lucas, S., and Possani, L.D. 2000. Tc1, from *Tityus cambridgei*, is the first member of a new subfamily of scorpion toxin that blocks K⁺-channels. *FEBS Lett.* 486: 117–120.
- Bax, A. and Davis, D.G. 1985. MLEV-17-based two-dimensional homonuclear magnetization transfer spectroscopy. *J. Magn. Reson.* 65: 355–360.
- Bontems, F., Roumestand, C., Boyot, P., Gilquin, B., Doljansky, Y., Menez, A., and Toma, F. 1991. Three-dimensional structure of natural charybotoxin in aqueous solution by 1H-NMR: Charybotoxin possesses a structural motif found in other scorpion toxins. *Eur. J. Biochem.* 196: 19–28.
- Brünger, A.T. 1998. *X-PLOR version 98*. Yale University Press, New Haven, CT.
- Catterall, W.A. 1980. Neurotoxins that act on voltage-sensitive sodium channels in excitable membranes. *Annu. Rev. Pharmacol. Toxicol.* 20: 15–43.
- Dauplais, M., Gilquin, B., Possani, L.D., Gomola-Briones, G., Roumestand, C., and Menez, A. 1995. Determination of the three-dimensional solution structure of toxistoxin: Analysis of structural differences with related short-chain scorpion toxins. *Biochemistry* 34: 16563–16573.
- DeBin, J.A., Maggio, J.E., and Strichartz, G.R. 1993. Purification and characterization of chlorotoxin, a chloride channel ligand from the venom of the scorpion. *Am. J. Physiol.* 264: 361–369.
- Doyle, D.A., Morais Cabral, J., Pfuetzner, R.A., Kuo, A., Gulbis, J.M., Cohen, S.L., Chait, B.T., and MacKinnon, R. 1998. The structure of the potassium channel: Molecular basis of K⁺ conduction and selectivity. *Science* 280: 69–77.
- Ellis, K.C., Tenenholz, T.C., Jerng, H., Hayhurst, M., Dullak, C.S., Gilly, W.F., Blaustein, M.P., and Weber, D.J. 2001. Interaction of a toxin from the scorpion *Tityus serrulatus* with a cloned K⁺ channel from squid (sqKv1A). *Biochemistry* 40: 5942–5953.
- Fernandez, I., Romi, R., Szendeffy, S., Martin-Eauclaire, M.F., Rochat, H., Van Rietschoten, J., Pons, M., and Giralt, E. 1994. Kallitoxin (1–37) shows structural differences with related potassium channel blockers. *Biochemistry* 33: 14256–14263.
- Garcia, M.L., Hanner, M., Knaus, H.G., Koch, R., Schmalhofer, W., Slaughter, R.S., and Kaczorowski, G.J. 1997. Pharmacology of potassium channels. *Adv. Pharmacol.* 39: 425–471.
- Goldstein, S.A., Phansau, D.J., and Miller, C. 1994. The charybotoxin receptor of a *Shaker* K⁺ channel: Peptide and channel residues mediating molecular recognition. *Neuron* 12: 1377–1388.
- Gomez-Lagunas, F., Olamendi-Portugal, T., Zamudio, F.Z., and Possani, L.D. 1996. Two novel toxins from the venom of the scorpion *Pandinus imperator* show that the N-terminal amino acid sequence is important for their affinities towards *Shaker*. *J. Membr. Biol.* 152: 49–56.
- Gouet, P., Courcelle, E., Stuart, D.I., and Metoz, F. 1999. ESPript: Analysis of multiple sequence alignments in PostScript. *Bioinformatics* 15: 305–308.
- Hyberts, S.G., Marki, W., and Wagner, G. 1987. Stereospecific assignments of side-chain protons and characterization of torsion angles in eglon c. *Eur. J. Biochem.* 164: 625–635.
- Johnson, B.A. and Sagg, E.E. 1992. Determination of the three-dimensional structure of iberitoxin in solution by 1H nuclear magnetic resonance spectroscopy. *Biochemistry* 31: 8151–8159.
- Johnson, B.A., Stevens, S.P., and Williamson, J.M. 1994. Determination of the three-dimensional structure of margatoxin by 1H, 13C, 15N triple-resonance nuclear magnetic resonance spectroscopy. *Biochemistry* 33: 15061–15070.
- Koradi, R., Billeter, M., and Wüthrich, K. 1996. MOLMOL: A program for display and analysis of macromolecular structures. *J. Mol. Graph.* 14: 51–5, 29–32.
- Kumar, A., Ernst, R.R., and Wüthrich, K. 1980. A two-dimensional nuclear Overhauser enhancement (2D NOE) experiment for the elucidation of complete proton-proton cross-relaxation networks in biological macromolecules. *Biochem. Biophys. Res. Commun.* 95: 1–6.
- Laskowski, R.A., Rullmann, J.A., MacArthur, M.W., Kaptein, R., and Thornton, J.M. 1996. AQUA and PROCHECK-NMR: Programs for checking the quality of protein structures solved by NMR. *J. Biomol. NMR* 8: 477–486.
- Marion, D. and Wüthrich, K. 1983. Application of phase sensitive two-dimensional correlated spectroscopy (COSY) for measurements of 1H-1H spin-spin coupling constants in proteins. *Biochem. Biophys. Res. Commun.* 113: 967–974.
- Meunier, S., Bernassau, J.M., Sabatier, J.M., Martin-Eauclaire, M.F., Van Rietschoten, J., Cambillau, C., and Darbon, H. 1993. Solution structure of P05-NH2, a scorpion toxin analog with high affinity for the apamin-sensitive potassium channel. *Biochemistry* 32: 11969–11976.
- Miller, C. 1995. The charybotoxin family of K⁺ channel-blocking peptides. *Neuron* 15: 5–10.
- Nicholls, A., Sharp, K.A., and Honig, B. 1991. Protein folding and association: Insights from the interfacial and thermodynamic properties of hydrocarbons. *Proteins* 11: 281–296.
- Proton, M., Saudek, V., and Sklenar, V. 1992. Gradient-tailored excitation for single-quantum NMR spectroscopy of aqueous solutions. *J. Biomol. NMR* 2: 661–665.
- Possani, L.D., Becerril, B., Delapierre, M., and Tytgat, J. 1999. Scorpion toxins specific for Na⁺-channels. *Eur. J. Biochem.* 264: 287–300.
- Rance, M., Sorensen, O.W., Bodenhausen, G., Wagner, G., Ernst, R.R., and Wüthrich, K. 1983. Improved spectral resolution in cosy 1H NMR spectra of proteins via double quantum filtering. *Biochem. Biophys. Res. Commun.* 117: 479–485.
- Romi-Lebrun, R., Lebrun, B., Martin-Eauclaire, M.F., Ishiguro, M., Escoubas, P., Wu, F.Q., Hisada, M., Pongs, G., and Nakajima, T. 1997. Purification, characterization, and synthesis of three novel toxins from the Chinese scorpion *Buthus martensii*, which act on K⁺ channels. *Biochemistry* 36: 1347–1348.

- Shieh, R.C., Chang, J.C., and Arreola, J. 1998. Interaction of Ba^{2+} with the pores of the cloned inward rectifier K^+ channels Kir2.1 expressed in *Xenopus* oocytes. *Biophys. J.* 75: 2313–2322.
- Sreerama, N. and Woody, R.W. 2000. Estimation of protein secondary structure from circular dichroism spectra: Comparison of CONTIN, SELCON, and CDSSTR methods with an expanded reference set. *Anal. Biochem.* 287: 252–260.
- Stamppe, P., Kolmakova-Paritsky, I., and Miller, C. 1994. Intimations of K^+ channel structure from a complete functional map of the molecular surface of charybdotoxin. *Biochemistry* 33: 443–450.
- Thompson, J.D., Higgins, D.G., and Gibson, T.J. 1994. CLUSTAL W: Improving the sensitivity of progressive multiple sequence alignment through sequence weighting, positions-specific gap penalties and weight matrix choice. *Nucl. Acids. Res.* 22: 4673–4680.
- Tytgat, J., Chandy, K.G., Garcia, M.L., Gutman, G.A., Martin-Estclair, M.F., van der Walt, J.J., and Possani, L.D. 1999. A unified nomenclature for short-chain peptides isolated from scorpion venom: α -KTx molecular sub-families. *Trends Pharmacol. Sci.* 20: 444–447.
- Valdivia, H.H. and Possani, L.D. 1998. Peptide toxins as probes of rymodine receptor structure and function. *Trends Cardiovasc. Med.* 8: 111–118.
- Valdivia, H.H., Martin, B.M., Escobar, L., and Possani, L.D. 1992. Noxiustoxin and leioritoxin III, two homologous peptide toxins with binding properties to synaptosomal membrane K^+ channels. *Biochem. Int.* 27: 953–962.
- Wishart, D.S., Sykes, B.D., and Richards, F.M. 1992. The chemical shift index: A fast and simple method for the assignment of protein secondary structure through NMR spectroscopy. *Biochemistry* 31: 1647–1651.
- Wüthrich, K. 1986. *NMR of protein and nucleic acids*. Wiley Interscience, New York, NY.

ลิขสิทธิ์มหาวิทยาลัยเชียงใหม่
Copyright© by Chiang Mai University
All rights reserved

Phosphorylation of the 24p3 Protein Secreted from Mouse Uterus *in Vitro* and *in Vivo*

Ying-Chu Lee,¹ Shyh-Dyh Lin,² Hui-Ming Yu,¹ Shui-Tein Chen,¹ and Sin-Tak Chu^{1,3}

Received August 10, 2001

The 24p3 protein is a 25 KDa glycoprotein, having been purified from mouse uterine fluid. Thr⁵⁴, Ser⁵⁸, and Thr¹²⁸:Ser¹²⁹ on the protein molecule were predicted to be the phosphorylation site of casein kinase II, protein kinase C, and cAMP-dependent protein kinase, respectively. Incorporation of phosphate to this protein from [γ -³²P]-ATP was tested in the solution suitable for the three kinases. Neither casein kinase II nor cAMP-dependent protein kinase reacted to the 24p3 protein; however, protein kinase C demonstrated phosphorylation to this protein. This phosphorylation may be competing with a polypeptide segment: Arg⁷⁹-Tyr-Trp-Ileu-Arg-Thr-Phe-Val-Pro-Ser⁵⁸-Ser-Arg-Ala-Gly-Glu-Phe-Thr-Leu-Gly⁹⁷ in the 24p3 protein molecule. To support this theory, Ser⁵⁸ is a phosphorylation site of protein kinase C on 24p3 protein. The enzyme kinetic parameter, based on the Michaelis-Menten equation, determined K_m to be 2.96 μ M in the phosphorylation of 24p3 protein by the kinase. Both of the phosphorylated and dephosphorylated form of 24p3 protein can enhance the cAMP-dependent protein kinase activity *in vitro*. In addition, this experiment will show for the first time that serine-phosphorylated 24p3 protein exists in mouse uterine tissue.

KEY WORDS: Phosphorylation; protein kinase; serinephosphate; uterine protein.

1. INTRODUCTION

A purified protein, derived from 24p3 cDNA, was originally by Hraba-Renevey *et al.* (1989) cloned from mouse kidney culture cells infected with polyoma virus-40, from mouse uterine luminal fluid (Chu *et al.*, 1996), and identified in the epididymis (Chu *et al.*, 2000). We identify this protein as 24p3, a 25 KDa glycoprotein, with a blocked N-terminus of pyroglutamate (Chu *et al.*, 1997). This protein is also present in lipopolysaccharide-stimulated PU5.1.8 macrophage (Meleus *et al.*, 1993) and bFGF-stimulated 3T3 cells (Davis *et al.*, 1991). The results of Liu and Nilson-Hamilton (1995) reveal it as an acute phase protein of liver. Based on a computer-assisted homologous search, it is classified as a member

of the lipocalin superfamily (Flower *et al.*, 1991). The protein also shows a high degree of similarity to human neutrophil gelatinase-associated lipocalin (NGAL) (70% identity) (Chu *et al.*, 1997; Kjeldsen *et al.*, 1993). Our previous results support a hydrophobic pocket of this protein molecule, showing it to be suitable for fatty acid and retinoid binding (Chu *et al.*, 1998). We also found that the epididymal 24p3 protein interacted predominantly with the acrosome of spermatozoa (Chu *et al.*, 2000). The biological function of this uterine protein remains unclear. This being evident, we are seeking further understanding of the function of the 24p3 protein.

Phosphorylation and dephosphorylation of protein is well-recognized as an important to regulate biological function. It may reflect a relationship between protein structure and biological activity. The phosphorylation or dephosphorylation of amino acid residue triggers struc-

¹ Institute of Biological Chemistry, Academia Sinica, Taiwan.

² Institute of Biochemical Science, College of Science, National Taiwan University, Taipei, 10617, Taiwan.

³ To whom correspondence should be addressed. Institute of Biological Chemistry, Academia Sinica, PO Box 23-106, Taipei, 10617, Taiwan. Tel: 886-2-23620261 (Ext. 4531); Fax: 886-2-23635038; e-mail: stc316@gate.sinica.edu.tw

⁴ Abbreviations: CKII, casein kinase II; NC, nitrocellulose; NGAL, neutrophil gelatinase-associated lipocalin; PKA, cAMP-dependent protein kinase; PKC, protein kinase C; PMSE, phenylmethyl sulfonyl; TFA, trifluoroacetic acid.

natural change in the molecules, altering their biological function (Kurosawa, 1994). The analysis of the primary structure of 24p3 protein suggests the presence of potential Ser/Thr sites for the phosphorylation by casein kinase II (CKII),⁴ protein kinase C (PKC), or cAMP-dependent protein kinase (PKA) (Fig. 1), thus further emphasizing the importance of verifying the phosphorylation in 24p3 protein. Accordingly, we investigated the phosphorylation of 24p3 protein by these three types of kinases.

Our results support a PKC phosphorylation site at Ser²⁵ but exclude both phosphorylation sites for CKII and PKA on the protein molecule. The K_m value is comparable to that reported for the most effective protein substrates for protein kinase C (Abe *et al.*, 1991). Use of the immunoprecipitation method to identify the serine-phosphorylated 24p3 protein in uterine tissue indicated the phosphorylation of 24p3 protein might be important and further established that the 24p3 protein enhanced the PKA activity *in vitro*.

2. MATERIALS AND METHODS

2.1. Materials

Outbred ICR mice were purchased from Charles River Laboratory (Wilmington, MA) and were bred in the animal center at the College of Medicine, National Taiwan University. All enzymes were purchased from Boehringer Mannheim G.m.b.H (Germany). Antiphosphoserine antibody and HRP-conjugated anti-rabbit IgG were obtained from Zymed Laboratories, Inc. (Cat no. 61-8100, CA, USA) and Promega (cat no. W4011, WI, USA), respectively. The 24p3 protein-induced antibody was prepared and partially purified with a protein A column, as per a previous method (Chiu *et al.*, 2000). The [γ -³²P]-ATP was from Amersham (Searle, Arlington Heights, IL). All other chemicals were reagent grade.

2.2. Prediction of Phosphorylation Sites

The method of matching consensus sequence patterns based on stepwise discrimination analysis was applied to seek the potential phosphorylation sites on the 24p3 protein molecule from a primary structure of the 24p3 protein. The analysis was executed by the computer program package PROSITE 9.1, which is (technically) interrelated to SWISS-PROT protein sequence data bank (Bairoch and Apweiler, 1997, 1998).

2.3. Solid-Phase Peptide Synthesis

Peptide was synthesized, via 4-(2,4-dimethoxyphenyl)-Fmoc-amino-methyl phenoxyl resin (0.281g, 0.89 mEq/g) with Fmoc-amino acid derivatives using an automatic peptide synthesizer (Applied Biosystem Model 433A, USA). After completion of synthesis, the peptide on resins were incubated with a cleavage mixture containing 0.75 g crystalline phenol, 0.25 mL 1,2-ethanedithiol, 0.5 mL thioanisole, 0.5 mL D.I. water, 10 mL trifluoro-

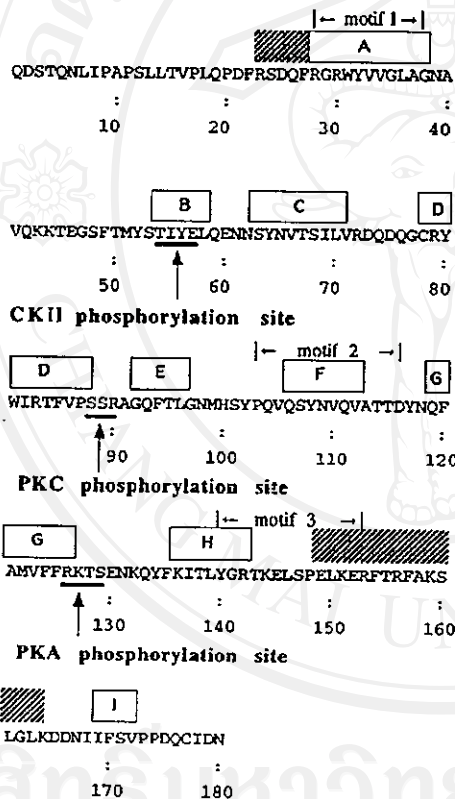


Fig. 1. The potential phosphorylation sites of protein kinases on 24p3 protein and its predicted secondary structure. Based on our previous report (Chiu *et al.*, 1998), the predicted secondary structures, which are conserved in the lipocalin protein superfamily (Monaco and Zanotti, 1992), are shown at the top of the sequence (β -strands A-I and helices in the hatch blocks). The three short motifs, which are highly conserved between members of the family (Flower *et al.*, 1991) are denoted. The consensus sequences for the phosphorylation site of different protein kinases are underlined and denoted.

Phosphorylation of the 24p3 Protein

565

acetic acid, for 90 min at room temperature, and the solvent was completely evaporated. The dry resin was then washed five times with 20 mL of cold ether. Synthetic peptide was then extracted by washing five times with 20 mL of 5% acetic acid. All extracts were lyophilized to yield a crude peptide (0.506g, 93.5% yield).

2.4. *In Vitro* Phosphorylation of 24p3 Protein

The [γ - 32 P]-ATP was diluted with unlabeled ATP, yielding a final specific activity of 0.5 Ci/mmol. In a specified solution reported previously (Gonzalez *et al.*, 1993; Hathaway and Traugh 1979; Glover *et al.*, 1983), 24p3 protein (5.0 μ g/mL) was phosphorylated by CKII (20 mU/mL), PKA (20 μ U/mL), or PKC (2 μ U/mL) in the presence of 0.2 nM radiolabeled ATP at 30°C for 5 min. The phosphorylation by PKC was processed in 20 mM HEPES containing 15.0 μ M phosphatidylserine, 1.3 mM CaCl_2 , 10 mM MgCl_2 , and 1.0 mM DTT at pH 7.4. The PKA phosphorylation was performed in 50 mM MES containing 10 mM MgCl_2 , 0.5 mM EDTA, and 1.0 mM DTT at pH 6.9. The CKII phosphorylation was carried out in 20 mM MES containing 130 mM KCl, 10 mM MgCl_2 , and 4.8 mM DTT at pH 6.9. The reaction mixtures were subjected to SDS/PAGE on a 15% polyacrylamide slab gel (0.075 \times 5.0 \times 6.0 cm). The gel was dried by a gel-dryer, then autoradiographed on x-ray film.

2.5. The Phosphorylation Activity of PKC and PKA

The PKC activity was assayed according to a phosphocellulose technique (Casnellie, 1991). In the specified solution, 24p3 protein (0–14 μ M), or synthetic polypeptide (0–2 μ M) comprising Arg⁷⁹-Tyr-Trp-Ilu-Arg-Thr-Phe-Val-Pro-Ser⁸⁹-Ser-Arg-Ala-Gly-Gln-Phe-Thr-Leu-Gly⁹⁷, of the protein molecule was incubated in the presence of PKC (2 μ U/mL) and 0.2 nM [γ - 32 P]-ATP at 30°C. The 10 μ L of aliquot was spotted onto a P81 phosphocellulose paper for 5 min and then baked for 40 min under a lamp. The paper was washed five times with 2.0 mL of 150 mM phosphoric acid, rinsed with alcohol for 2 min, and baked dry. The radioactivity on the papers was counted by a β -counter. The velocity of 32 P-incorporation to the protein substrate was fitted to a double reciprocal plot constructed from the Michaelis-Menten equation.

The established method of Goueli *et al.* (1995), the cAMP-dependent protein kinase activity, was carried out in a 25 μ L reaction mixture containing 40 mM Tris-HCl, pH 7.4, 20 mM MgCl_2 , 100 μ M [γ - 32 P]-ATP,

100 μ g/mL BSA, and 100 μ M biotinylated peptide substrate (Leu-Arg-Arg-Ala-Ser-Ileu-Gly) (V7480, Promega, WI, USA). The reaction mixture was preincubated at 30°C for 5 min, followed by 37°C for 5 min. At each treatment, a 10- μ L aliquot was spotted on a streptavidin-conjugated membrane and washed with 2 M NaCl. This washing process was repeated four times, followed by an additional four times washing with 1% H_3PO_4 containing 2M NaCl, and twice with distilled water to remove the free isotope impurities. The membranes were then dried and counted using a liquid scintillation counter.

2.6. Phosphorylation and Dephosphorylation of 24p3 Protein

The purified 24p3 protein of uterine luminal fluid was prepared according to our previous method (Chu *et al.*, 1996). Fifty μ g of 24p3 protein was mixed with 300 μ U of bovine placenta alkaline phosphatase in 200 μ L 0.1 M glycine, pH 10.4, containing 0.1 M NaCl, 50 mM MgCl_2 , 1.0 mM DTT, 2.0 mM EDTA, and 100 μ M phenylmethyl sulfonyl fluoride (PMSF). The mixture was incubated at 30°C for 4 h to remove the phosphate from protein. After the dephosphorylation, 60 μ L 0.2 N HCl was added to neutralize and the mixture was fractionated by reversed-phase HPLC, with a 35% to 45% linear gradient of acetonitrile in 0.1% trifluoroacetic acid (TFA), and a flow rate of 0.7 mL/min on a C18, 7 micron, 250 \times 4.6 mm column (Macherey-Nagel, GmbH & Co., KG). The dephosphorylated 24p3 protein was collected manually and lyophilized.

To phosphorylate the protein, 30 μ g 24p3 protein was mixed with 50 ng PKC in 100 μ L of 20 mM Tris-HCl, pH 7.5, containing 10 mM MgCl_2 , 0.2 mM CaCl_2 , 3 μ g/ μ L phosphatidylserine, 1 μ g/ μ L 1,2-dioleoyl-sn-glycerol, 100 μ M Na_2VO_4 , and 100 μ M PMSF. The reaction mixture was incubated at 37°C for 1 h to ensure the phosphorylation reaction. After the reaction, the phosphorylated 24p3 protein was fractionated by reversed-phase HPLC, as with the previous method. Phosphorylated 24p3 protein was then collected manually and lyophilized. The dephosphorylation/phosphorylation 24p3 protein was analyzed by Western-blot analysis with an antiphosphoserine antibody.

2.7. *In Vivo* Phosphorylation Determination

Mature female mice (6 to 8 weeks) at proestrus phase were sacrificed by cervical dislocation and their uteri removed. The uteri were homogenized in a solution

containing 20 mM Tris-HCl, pH 7.4, 1 mM EDTA, 25 mM NaF, 0.1 μ M okadaic acid, 2 mM Na_2VO_4 , and 2.5 mM β -glycerophosphate to extract the proteins, and then centrifuged at $360,000 \times g$ for 40 min to remove the debris. The extraction mixture also contained 1X dilution of protease inhibitor cocktail, (PI Cocktail, Cat No. 1697498, Roche Molecular Biochemicals, Germany). The supernatant was then obtained as a tissue homogenate extract. Using the Dynabeads immunomagnetic system to isolate the 24p3 protein from tissue extract, a target antigen-antibody complex can be isolated with an indirect technique. With the indirect technique, a sheep anti-rabbit IgG, specific for the IgG-antigen complex, is coupled to the Dynabeads M-280 (Dyna, cat No. 112.03, Dynal A. S. Oslo, Norway). The coated beads are then used to capture the desired target of protein complex. The homogenate extract containing 24p3 protein (3 mg) is incubated with the 24p3 protein-induced antibody (3 μ g) for 2 h at 4°C, while gently agitating with a rotator. This procedure allows for the antigen-antibody complex formation to be completed. The antigen-antibody complex can now be isolated by incubation with 50 μ L Dynabeads M-280 sheep anti-rabbit IgG for 1 h at 4°C. After the incubation, a magnet is applied on the wall of the test tube for 1 min, isolating the target. A 10 μ L electrophoresis sample buffer is added and boiled for 5 min, and then centrifuged at $6000 \times g$ for 1 min to remove the beads. The dissolved proteins in the sample buffer were resolved by SDS/PAGE [15% (w/v) acrylamide] on a gel slab. Proteins were transferred from gel to a nitrocellulose (NC) membrane in PBS at 4°C for 32 h by the diffusion method (Bowen *et al.*, 1980). The transferred proteins were detected with antiphosphoserine antibody (diluted to 1.25 μ g/10 mL), or 24p3 protein antibody (diluted to 2 μ g/15 mL), followed by HRP-conjugated anti-rabbit IgG diluted to 1:12000 and fluorography. The reactive bands were visualized using an enhanced chemiluminescence (ECL) kit (RPN 2132, Amersham Pharmacia Biotech U.K. Ltd) and exposed on x-ray film.

3. RESULTS

3.1. Phosphorylation of 24p3 Protein by Kinases

Fig. 1 shows the motif search for the consensus sequences of protein kinase phosphorylation sites on the 24p3 protein molecule. Based on our previous report (Chu *et al.*, 1998), both the predicted secondary structure, including the three short motifs, are highly conserved in the lipocalin protein superfamily (Monaco and

Zanotti, 1992), and are deciphered in Fig. 1. The Thr⁵⁴-Ile-Tyr-Glu⁵⁷, Ser⁸²-Ser-Arg⁹⁰, and Arg¹²⁴-Lys-Thr-Ser¹²⁹ matched with the consensus sequences for the phosphorylation site of CKII, PKC, and PKA, respectively. The three peptide segments are not included in the three short, highly conserved lipocalin family motifs. The first one is inside β -strand B, the second in a less rigid conformation and may be in a β -turn or in unordered region between β -strands D and E. Part of the third is overlapped with β -strand G. The ability of these protein kinases to phosphorylate Thr⁵⁴, Ser⁸², and Thr¹²⁰/Ser¹²⁹ was examined. The progressive result of the ³²P-incorporation from [γ -³²P]-ATP to the proteins in the specified solution for each kinase at 30°C for 5 min is determined by β -counter. Fig. 2A displays the

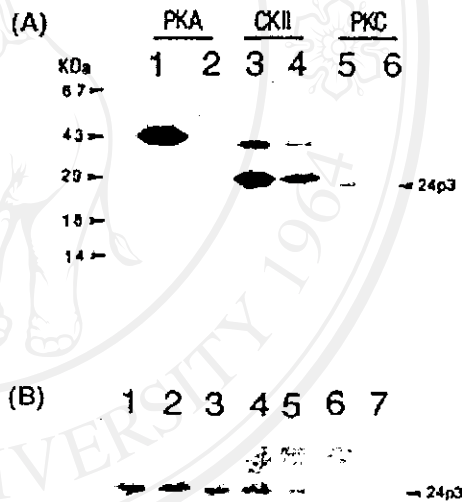


Fig. 2. *In vitro* phosphorylation of 24p3 protein by kinases. (A) Each kinase was incubated alone (lanes 2, 4, 6) or in the presence of the 24p3 protein (lanes 1, 3, 5) and the ³²P-incorporation to the protein (20 μ M) was detected on the autoradiogram after the reaction mixture had been resolved by SDS/PAGE on a 15% polyacrylamide gel slab (see text for details). (B) 24p3 Protein (20 μ M) was incubated with PKC (2 mU/mL) in the presence of [γ -³²P]-ATP (0.5 Ci/mmol) and a synthetic polypeptide comparing Arg⁷⁹-Tyr-Tip-Ilu-Arg-Thr-Phe-Val-Pro-Ser⁸⁴-Ser-Arg-Ala-Gly-Gln-Phe-Thr-Leu-Gly⁹⁷ in the protein at 30°C for 5 min. The reaction mixture was resolved by SDS/PAGE and the extent of ³²P-incorporation to the 24p3 protein was compared following autoradiography. The molar ratio of the synthetic polypeptide to the 24p3 protein in the incubation was: 0 (lane 1), 1.0 (lane 2), 2.0 (lane 3), 5.0 (lane 4), 10.0 (lane 5), 20.0 (lane 6), 40.0 (lane 7).

Phosphorylation of the 24p3 Protein

567

autoradiogram of ^{32}P -labeled proteins after the reaction mixtures were resolved by SDS-PAGE; these protein kinases could be distinguished by their migration on SDS-PAGE. PKA appeared as a 41 kDa band and PKC as a 82 kDa band. CKII was resolved into one 42 kDa α -subunit and one 26 kDa β -subunit. Neither PKA nor PKC but both subunits of CKII became radiolabeled when each kinase was isolated and incubated (cf. lanes 2, 4, and 6, of Fig. 2A), indicating that the autophosphorylation occurred only at both subunits of CKII among the three protein kinases. PKA showed no activity to phosphorylate 24p3 protein but the kinase became phosphorylated by the presence of 24p3 protein during incubation (cf. lanes 1 and 2, of Fig. 2A). The autophosphorylation of both subunits of CKII was enhanced by 24p3 protein, although the enzyme did not phosphorylate 24p3 protein (cf. lanes 3 and 4 of Fig. 2A). One radiolabeled protein band corresponding to 24p3 protein was detected in the incubation of PKC with 24p3 protein (cf. lanes 5 and 6 of Fig. 2A), indicating that PKC is able to phosphorylate 24p3 protein. Because Ser⁷⁹ is a predicted phosphorylation site of PKC, the interaction between PKC and a synthetic polypeptide comprising Arg⁷⁹-Tyr-Trp-Ilu-Arg-Thr-Phe-Val-Pro-Ser⁸⁰-Ser-Arg-Ala-Gly-Gln-Phe-Thr-Leu-Gly⁹⁷ in the 24p3 protein molecule was further investigated. The ^{32}P -incorporation of $[\gamma\text{-}^{32}\text{P}]\text{-ATP}$ to 24p3 protein is suppressed by the presence of this polypeptide. The results of one representative experiment (shown in Fig. 2B) indicates a decrease 24p3 protein phosphorylation coincided with the increase in the molar ratio of the polypeptide to 24p3 protein in the reaction. When the molar ratio was more than 20, the 24p3 protein was unable to be phosphorylated.

3.2. Phosphorylation Kinetic of PKC on the 24p3 Protein

The velocity of phosphate incorporation from ATP to the protein substrates by the PKC phosphorylation has been determined (Fig. 3A), and the kinetic parameters were obtained from the double reciprocal plot, based on Michaelis-Menten equation (Fig. 3A, inset). K_m was estimated at 2.96 and 0.42 μM for phosphorylation of 24p3, or the synthetic polypeptide, respectively (Fig. 3B). It is surprising to note that the phosphorylation of the synthetic polypeptide occurs more rapidly than that of the 24p3 protein due to the phosphorylation site on the synthetic polypeptide being less rigid, and it becomes more susceptible to the enzyme catalysis.

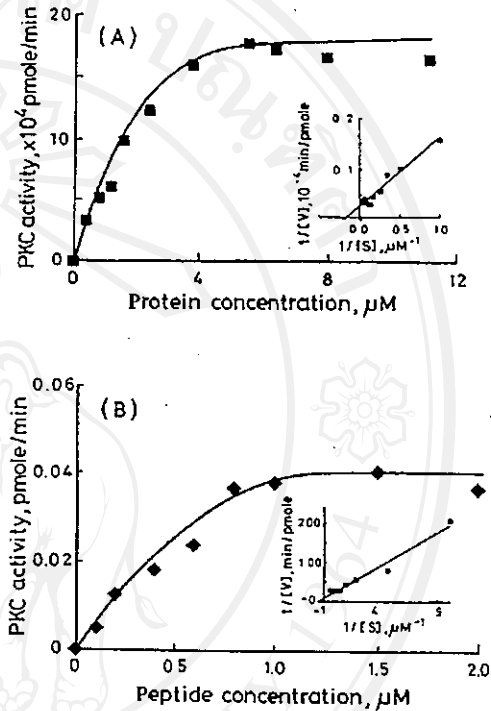


Fig. 3. The kinetics of PKC for the phosphorylation of 24p3 protein. The 24p3 Protein (0–14 μM) or the synthetic polypeptide (0–2 μM) was incubated with PKC (2 $\mu\text{U/mL}$) in the presence of $[\gamma\text{-}^{32}\text{P}]\text{-ATP}$ at 30°C. The rate of ^{32}P -incorporation to 24p3 protein (A) or the synthetic polypeptide (B) was measured. The double reciprocal plot based on the Michaelis-Menten equation is given in the inset.

3.3. The 24p3 Protein Enhances PKA Activity

Fig. 4 shows the dose-relationship activity for PKA in the presence of the 24p3 protein. Comparing the PKA activity in the absence of 24p3 protein solution (Fig. 4 □) with the presence of phosphorylated (Fig. 4 ■), or unphosphorylated 24p3 protein (Fig. 4 ◻) in the incubation medium, sufficiently increased the PKA activity by 1.25- to 5-fold, because the 24p3 protein molar ratio was increased by 10- to 100-fold (Fig. 4A–E). Although the PKA activity in the presence of dephosphorylated 24p3 protein showed few enhancements than in the presence of phosphorylated form, both forms enhanced the PKA activity.

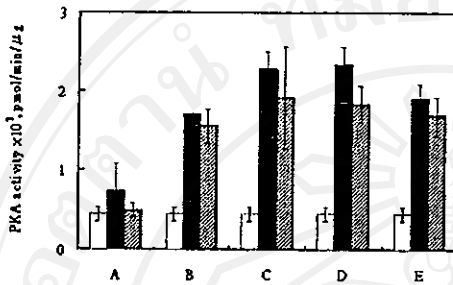


Fig. 4. Effect of 24p3 protein on the PKA activity. The 0.25 pmole PKA activity was determined (cf. Methods) in absence (□) or presence of phosphorylated (■) or unphosphorylated 24p3 protein (▨). Amount of added 24p3 protein: A. 2.5 pmole; B. 5.0 pmole; C. 10.0 pmole; D. 12.5 pmole; E. 25.0 pmole. Each value represents the mean \pm SEM of triplicates from a representative experiment.

3.4. Detection of Phosphoserine in 24p3 Protein from Mouse Uteri

The 24p3 protein can be phosphorylated *in vitro* by PKC at the same site as observed *in vivo*, as judged by Dynabeads immunoprecipitation. The serinephosphate on the NC membrane has shown that the 24p3 protein in the immunoprecipitate is phosphorylated *in vivo* (lane 2, Fig. 5B). As shown in Fig. 5 (panel A), the precipitated 24p3 protein was verified by 24p3 protein induced antibody at uterine tissue (lane 2) and purified 24p3 protein as a control (lane 1). Comparing the result of lane 1 with lane 2 in Fig. 5B, the phosphorylated-serine is absent in the purified-24p3 protein; dephosphorylation might occur in uterine luminal fluid or during purified process. The weakly fluorescent band of anti-rabbit IgG, shown in panel C (Fig. 5B), indicates the antiphosphoserine antibody reacted specifically to phosphoserine of the 24p3 protein. Using alkaline phosphatase to dephosphorylate the precipitate taken from uterine tissue with an antibody for the 24p3 protein showed only a dim fluorescent band by the antiphosphoserine antibody, which supports the existence of *in vivo* phosphorylation of the 24p3 protein (data not shown).

4. DISCUSSION

Our observations have shown that an apparent K_m in the PKC phosphorylation of the 24p3 protein (2.96 μM) is comparable to that hitherto reported as the most effective protein substrates for PKC (0.3–9.7 μM) (Abe *et al.*, 1991). The likelihood of phosphorylating 24p3 protein by PKC *in vivo* is conceivable. Our study of *in vitro* and



Fig. 5. Immunodetection of phosphorylated 24p3 protein in uterine tissue. Mouse uterine tissues were collected (cf. Methods). The 24p3 protein was immunoprecipitated from uterine tissue and analyzed by Western-blot analysis with antibody against 24p3 protein or phosphoserine. Lane 1 is purified 24p3 protein as a control. Lane 2 is the immunoprecipitated protein from mouse uterine tissue. Panel A, detected by 24p3 protein induced antibody; panel B, detected by antiphosphoserine antibody; panel C, detected by anti-rabbit IgG antibody as a control.

in vivo phosphorylation suggests PKC phosphorylation suggests PKC phosphorylation on phosphoserine of 24p3 protein does exist in this uterine protein. The result shown in Fig. 2A, lane 1, suggests that the 24p3 protein induces the conformational change of PKA and facilitates the autophosphorylation of the PKA. The phenomenon of autophosphorylation has been noted in many protein kinases, such as cAMP-dependent protein kinase II (Rubin and Rosen, 1975). The potential role of such autophosphorylation to alter activity of the kinase has been suggested in many reports. The enhancement of enzymatic activity may result from the 24p3 protein association, thus causing the conformational change of PKA. Based on the results (Fig. 2, lane 1; Fig. 4), it is reasonable to speculate that the 24p3 protein may have induced the conformational change of PKA to facilitate the autophosphorylation and then induced the enzymatic activity. The phenomenon of phosphorylation on 24p3 protein may not correlate to PKA activity directly. In the present study, the CKII activity was not affected by 24p3 protein (data not shown).

even if the 24p3 protein increased autophosphorylation of CKII. Elucidation of the interrelationship between 24p3 protein and PKA is more worthy to elucidate. Further studies are necessary to determine if enhancement of PKA activity will occur *in vivo*.

In summary, we show for the first time that 24p3 protein is a serine phosphorylated-glycoprotein in mouse uteri. The phosphorylation and glycosylation, the post-translational modifications of a protein, which have optional, affect the activity of secretion (Kukuruzinska and Lemm, 1998; Price *et al.*, 1994). As a secretory protein, whether phosphorylation (in this paper) or glycosylation (Chu *et al.*, 1996) of the 24p3 protein are a necessary requirement for the secretion of the 24p3 protein from the tissue will require future study. Because the phosphorylation-dephosphorylation of a lipid-binding protein may regulate the directional orientation of lipid flux in cells (Bueli *et al.*, 1992) as a lipocalin of 24p3 protein (Chu *et al.*, 1997), the study of phosphorylation of the 24p3 protein is important. Phosphorylation may represent a mechanism, which regulates a 24p3 protein association with the hydrophobic molecule and regulates biological activity of the 24p3 protein. The outcome may determine how the phosphorylation role is identified in the hydrophobic molecule interaction or protein secretion. Based on the result of the autoradiogram study, the fact that the 24p3 protein facilitated the autophosphorylation, of PKA and enhanced the PKA activity, indicating an interrelation between the 24p3 protein and kinase *in vivo*, merits further attention. Further study is needed to elucidate the significance of the 24p3 protein within the reproductive system.

ACKNOWLEDGMENT

This work was partially supported by grant NSC89-2311-B001-064 from National Sciences Council, Taiwan.

REFERENCES

- Abe, K., Sakuke, K., Tanaka, M., Uehara, Y., Matsuno, K., Miyazaki, T., and Katoh, N. (1991). *Biochem. Biophys. Res. Commun.* **176**, 1123-1129.
- Bairoch, A. and Apweiler, R. (1997). *J. Mol. Med.* **75**, 312-316.
- Bairoch, A. and Apweiler, R. (1998). *Nucleic Acids Res.* **26**, 38-42.
- Bowen, B., Steinberg, J., Laemmli, V. K., and Weinraub, H. (1980). *Nucleic Acid Res.* **8**, 1-20.
- Bueli, M. K., Xu, Z., Banaszak, L. J., and Bernlohr, D. A. (1992). *Biochemistry* **31**, 3493-3499.
- Casuelle, J. E. (1991). *Meth. Enzymol.* **200**, 115-120.
- Chu, S. T., Huang, H. L., Chen, J. M., and Chen, Y. H. (1996). *Biochem. J.* **316**, 545-550.
- Chu, S. T., Lin, H. J., and Chen, Y. H. (1997). *J. Peptide Res.* **49**, 582-585.
- Chu, S. T., Lin, H. J., Huang, H. L., and Chen, Y. H. (1998). *J. Peptide Res.* **52**, 390-397.
- Chu, S. T., Lee, Y. C., Nein, K. M., and Chen, Y. H. (2000). *Mol. Reprod. Dev.* **57**, 26-36.
- Davis, T. R., Tabatabai, L., Bruins, K., Hamilton, R. T., and Nilsen-Hamilton, M. (1991). *Biochem. Biophys. Acta* **1095**, 145-152.
- Flower, D. R., North, A. C. T., and Attwood, T. K. (1991). *Biochem. Biophys. Res. Commun.* **180**, 69-74.
- Glover, C. V., Shelton, E. R., and Brutlag, D. L. (1983). *J. Biol. Chem.* **258**, 3258-3265.
- Gonzalez, A., Klauun, E., Sessoms, J. S., and Chen, S. J. (1993). *Anal. Biochem.* **215**, 184-189.
- Goueli, B. S., Hsiao, K., Tereba, A., and Goueli, S. A. (1995). *Anal. Biochem.* **225**, 10-17.
- Hathaway, G. M. and Traugh, J. A. (1979). *J. Biol. Chem.* **254**, 762-768.
- Hraba-Renevey, S., Turler, H., Kress, M., Salomon, C., and Weil, R. (1989). *Oncogene* **4**, 601-608.
- Kjeldsen, L., Jonsen, A. H., Sengelov, H., and Borregaard, N. (1993). *J. Biol. Chem.* **268**, 10425-10430.
- Kukuruzinska, M. A. and Lemmon, K. (1998). *Crit. Rev. Oral Biol. Med.* **9**, 415-448.
- Kurosawa, M. (1994). *J. Pharmacol. Toxicol. Meth.* **31**, 135-139.
- Liu, Q. and Nilsen-Hamilton, M. (1995). *J. Biol. Chem.* **270**, 22565-22570.
- Meheus, L. A., Fransen, L. M., Raynackers, J. G., Blockx, H. A., van Beeumen, J. J., van Bui, S. M., and van de Voorde, A. (1993). *J. Immunol.* **151**, 1535-1547.
- Monaco, H. L. and Zanotti, G. (1992). *Biopolymers* **32**, 457-465.
- Price, P. A., Rice, J. S., and Williamson, M. A. (1994). *Prot. Sci.* **3**, 822-830.
- Rubin, C. S. and Rosen, O. M. (1975). *Annu. Rev. Biochem.* **44**, 831-887.



Enhancing the hypotensive effect and diminishing the cytolytic activity of hornet mastoparan B by D-amino acid substitution

Chewn-Lang Ho^{*}, Yan-Ping Shih, Kung-Tsung Wang, Hui-Ming Yu

Institute of Biological Chemistry, Academia Sinica, Nankang, Taipei 115, Taiwan

Received 24 November 2000; accepted 6 April 2001

Abstract

Mastoparan B (MP-B) is a cationic tetradecapeptide (LKLSIVSWAKKVL-CONH₂) isolated from the venom of the Taiwan hornet *Vespa basalis*. Unlike other vespid mastoparans, the peptide is capable of inducing short-term hypotension and causes hemolysis in animals. This study was aimed to find out MP-B analogs that possess higher hypotensive potency with the least lytic action by D-amino acid substitution, especially at lysine (Lys) residues. The synthetic MP-B isomer in which Lys² was replaced by D-Lys showed a significant decrease in both hemolytic and hypotensive activities. Substitution of Lys⁴ by D-Lys in MP-B also caused a marked reduction of hemolytic activity, but its hypotensive action was only slightly affected. However, when Lys^{11,12} were replaced by D-Lys, the resulting isomer ([D-Lys^{11,12}]MP-B) exhibited a higher hypotensive activity with negligible hemolytic activity as compared with the native peptide. The D-antipod of MP-B in which all amino acid residues were replaced by D-isomers showed the highest hypotensive activity with a hemolytic activity about 1/5 that of MP-B. The results reveal that D-Lys substitution at the N-terminus of MP-B (Lys^{2,4}) causes decreases in both hypotensive and hemolytic activities, while D-Lys substitution at the C-terminus (Lys^{11,12}) leads to a significant increase in hypotensive activity of MP-B with a remarkable decrease in hemolytic activity. The hypotensive effect of [D-Lys^{11,12}]MP-B was more prominent on spontaneously hypertensive rats. At a proper dose (0.3 mg/kg) the peptide could reduce the high blood pressure (~180 mm Hg) of the rat to a normal level (~120 mm Hg) for more than 3 h. [D-Lys^{11,12}]MP-B which possesses a potent hypotensive action with the least cytolytic side effect is the best MP-B analog for studying the mechanism of cardiovascular inhibition by MP-B and could be useful as a hypotensive agent in hypertension crisis. © 2001 Elsevier Science Ltd. All rights reserved.

1. Introduction

Mastoparans, the mast-cell-degranulating peptides of the vespid venoms, are the major peptide components in many species of hornets (Nakajima, 1984). Mastoparan B (MP-B) is a cationic tetradecapeptide (LKLSIVSWAKKVL-CONH₂) isolated from the venom of the hornet *Vespa basalis*, which is the most dangerous species of hornet found in Taiwan (Ho and Hwang, 1991). In addition to having the conserved lysine structure (Lys^{1,11,12}) of vespid mastoparans, MP-B has an extra-lysine at position 2 and a unique tryptophan at position 9 in its sequence. Although several mastoparan homologs have been isolated and characterized as liberators of histamine from mast cells (Nakajima, 1984;

Pick, 1984; Nakajima, 1986), only MP-B has been found to induce short-term hypotension in rats (Ho et al., 1994). The hypotensive effect of MP-B was inhibited by cyproheptadine (anti-serotonin) and reserpine (amine-depleting agent), but not by diphenhydramine (antihistamine). The site(s) and molecular mechanism of the hypotensive action induced by MP-B remain to be elucidated. On the other hand, MP-B has also been found to possess hemolytic activity on the red cells of guinea-pigs and rats (Ho and Hwang, 1991). The hypotensive effect of MP-B may be useful as a tool to study its mechanism of action, or used as a hypotensive agent for research, if its potency (degree and the duration of action) could be increased and its hemolytic activity reduced. Previous studies on the structure and activity relationship of MP-B have revealed that some lysine residues are critical for the hypotensive effect of the peptide (Ho et al., 1994), while tryptophan is responsible for its hemolytic activity (Ho et al., 1996). Here we report that a synthetic D-isomer

^{*} Corresponding author. Tel.: +886-2-2785-5696; fax: +886-2-2788-9759.

E-mail address: hoel@sinica.edu.tw (C.-L. Ho).

of MP-B in which lysine 11 and 12 were replaced by D-amino acids ([D-Lys^{11,12}]MP-B) showed a significantly higher hypotensive potency with negligible hemolytic activity as compared with native MP-B.

2. Materials and methods

The hornet venom was collected by pressing the venom sacs dissected from the ether-anesthetized worker hornets of *Vespa basalis* which were captured from the mountain area of east Taiwan (Haulien County).

Isolation of native MP-B from hornet venom was performed on a gel-filtration column (Fractogel TSK HW-50S, 2.6 × 45 cm, E. Merck, Germany) eluted with ammonium acetate buffer (0.05 M, pH 5.5). The isolated peptide was further purified using a cation-exchange column (CM-Trisacryl M, 1.0 × 20 cm, IBF Biotechnics, France) eluted with a linear gradient of ammonium acetate (0.05 M at pH 5.5, to 1.0 M at pH 6.8) as described previously (Ho and Hwang, 1991).

Mastoparan B and its D-isomers were synthesized via 4-(2', 4'-dimethoxyphenyl)-Fmoc-aminomethyl-phenoxyl resin with Fmoc-amino acid derivatives by an automatic peptide synthesizer (Applied Biosystem Model 431A, USA) as described previously (Yu et al., 1993). The crude peptide was first eluted through a gel-filtration column (Fractogel TSK HW-40S, 2.6 × 45 cm) with ammonium acetate buffer (0.1 M, pH 5.5) and purified by rechromatography on a reverse-phase HPLC column (Vydac C18, 1.0 × 25 cm, USA) followed by a second gel-filtration chromatograph on the same TSK column eluted with the same buffer at a higher pH (0.1 M ammonium acetate, pH 8.0). The yield of the purified peptide (purity > 97%) was 35–41% (w/w) of the input materials. The primary structures of the synthetic peptides were confirmed by both sequence analysis (Applied Biosystem 477A sequencer, USA) and mass determination (fast-atom-bombardment mass spectrometer, JEOL SX-102A, Japan) as shown in Table 1.

The hypotensive effect of the peptides was studied on Wistar male rats (200–250 g) and spontaneously hypertensive rats (SHR, 240–260 g) anesthetized with sodium pentobarbital (45 mg/kg, i.p.). Arterial blood pressure was

recorded from the femoral artery with a Statham P23 AC pressure transducer attached to a circulation system computer (Cardiomax-II, Columbus Instrument, Ohio, USA) and a Gould TA24 recorder. A standard lead II electrocardiogram (ECG) was recorded simultaneously. MP-B and its D-isomers were injected from the femoral vein.

Direct hemolytic activity of MP-B and its D-isomers was assayed on washed red blood cells of the guinea-pig. Washed red blood cells were prepared from blood withdrawn from the guinea-pig by repeated suspension and centrifugation (1000 rpm) as described (Ho and Hwang, 1991). The red blood cells (1%) were incubated with the peptides in Tris-buffered (0.01 M, pH 7.4) saline (0.15 M, NaCl) at 37°C for 60 min as described previously (Wu et al., 1982). Hemolytic action was stopped by addition of cooled (4°C) Tris-buffered saline and the degree of hemolysis was measured by the released hemoglobin at a wavelength of 540 nm. The statistical significance of the data was determined by unpaired Student's *t*-test.

The circular dichroism (CD) spectra of MP-B and its D-isomers were recorded with a CD spectrometer (Jasco J-720, Japan). The peptides were dissolved in Tris-buffered saline containing 20% trifluoroethanol. The $[\theta]$ values were expressed as the molar ellipticity of the peptides.

3. Results

3.1. Hypotensive effect of MP-B and its D-isomers on normotensive Wistar rats

In order to search for MP-B isomers with high hypotensive potency and low cytotoxicity, a series of D-Lys substituted isomers and a all-D isomer of MP-B (D-MP-B) were synthesized (Table 1). Mastoparan B isolated from hornet venom caused a short-term decrease in arterial blood pressure in rats. The hypotensive effect of MP-B was dose-dependent in both the degree and duration of hypotension (Fig. 1). The fall in mean arterial blood pressure measured 10 min after i.v. injection of MP-B at doses of 0.5 and 1.0 mg/kg were 19.7 ± 6.2 and 52.2 ± 4.6 mm Hg (mean ± SEM, *n* = 4), respectively. Injection of D-MP-B at a dose of 0.5 mg/kg induced a

Table 1
Amino acid sequences and retention times of mastoparan B and its D-isomers

Peptide	Amino acid sequence	Retention time (min) ^a
MP-B	L K L K S I V S W A K K V L · CONH ₂	26.8
D-MP-B	D-L D-K D-L D-K D-S D-I D-V D-S D-W D-A D-K D-K D-V D-L · CONH ₂	26.8
[D-Lys ²]MP-B	L D-K L K S I V S W A K K V L · CONH ₂	25.7
[D-Lys ¹]MP-B	L K L D-K S I V S W A K K V L · CONH ₂	25.4
[D-Lys ^{11,12}]MP-B	L K L K S I V S W A D-K D-K V L · CONH ₂	22.0

^a Retention times were obtained by reverse-phase HPLC with a Vydac C₁₈ column (1.0 × 25 cm) eluted with a linear gradient of acetonitrile (20–70%, v/v) containing 6 mM trifluoroacetic acid. The purity of the synthetic peptides was higher than 97%.

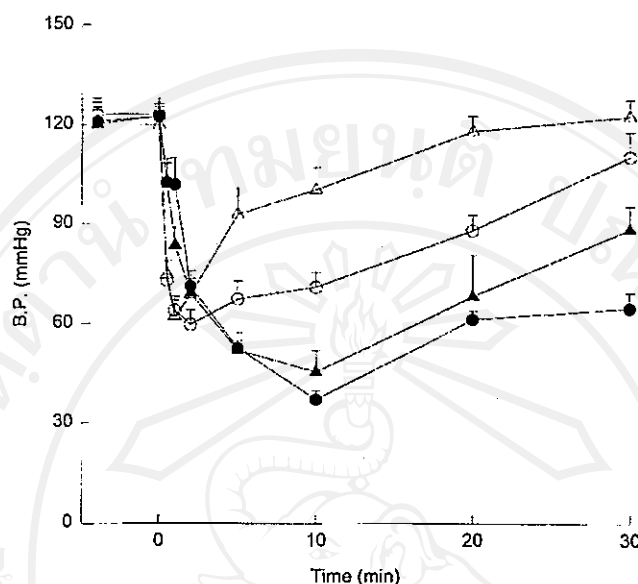


Fig. 1. Dose-dependent decreases in arterial blood pressure induced by different doses of MP-B and its all-D isomer in rats. MP-B (Δ , 0.5 mg/kg; \circ , 1.0 mg/kg) or D-MP-B (\blacktriangle , 0.5 mg/kg; \bullet , 1.0 mg/kg) was injected via the femoral vein at zero time and mean blood pressure (B.P.) was measured as described in Materials and Methods. Each point represents mean \pm SEM of three to four animals.

hypotensive effect that was significantly more potent (both the degree and duration of fall in blood pressure) than that induced by its L-isomer at two-fold that dose (Fig. 1). The decrease in mean blood pressure measured at 10 min after injection of D-MP-B (0.5 mg/kg) was 77.4 ± 7.3 mm Hg ($n=3$) with a duration much longer (>60 min) than that provoked by the same dose of its L-isomer (~ 30 min). Mastoparan B has four Lys residues located at the positions 2, 4, 11 and 12 of the peptide. Lys² and Lys¹¹ or Lys¹² have been found to be crucial for the hypotensive effect of MP-B (Ho et al., 1994). The substitution of Lys² by D-Lys in MP-B caused a decrease in its hypotensive action, while the replacement of Lys^{11,12} by D-Lys caused a marked increase in its hypotensive action (Fig. 2). At the dose of 0.5 mg/kg, the hypotensive effect of [D-Lys^{11,12}]MP-B was significantly higher than that induced by the native peptide and quite similar in potency to that provoked by D-MP-B. The substitution of Lys² by D-Lys in MP-B did not cause a significant change in the degree of maximal fall of blood pressure. However, the rate of recovery was changed. The treated rat tended to maintain a blood pressure lower than the control value for more than 60 min (Fig. 2). All D-isomers of MP-B except [D-Lys²]MP-B caused a more sustained hypotensive effect in rats as compared with its L-isomer.

3.2. Hypotensive effect of [D-Lys^{11,12}]MP-B on SHR rats

The hypotensive effect of the D-isomer of MP-B was

more prominent on spontaneously hypertensive rats (SHR strain). A typical example is given in Fig. 3. The SHR rat showed a mean arterial blood pressure around 180 mm Hg. Injection of [D-Lys^{11,12}]MP-B at a dose of 0.3 mg/kg caused a decrease of blood pressure from 180 to about 55 mm Hg in 5 min followed by rapid rise to about 100 mm Hg in 30 min. Thereafter, the treated rat could maintain its blood pressure at a normal level (around 120 mm Hg) for another 3 h or more. At higher dose (0.5 mg/kg), the peptide caused a fall of blood pressure to less than 40 mm Hg in 10–20 min followed by gradually rise to 65 mm Hg in 60 min. The treated rat showed a relatively low blood pressure (70–90 mm Hg) for the rest of the experimental period (Fig. 3). Significant decreases in heart rates (control value 406 ± 18 min⁻¹, $n=4$) were not found in SHR rats treated with 0.3 mg/kg of the peptide observed 30 min after the peptide treatment (380 ± 4 and 397 ± 9 min⁻¹ at 1 and 3 h, respectively). Therefore, 0.3 mg/kg appears to be an appropriate dose of [D-Lys^{11,12}]MP-B for reducing the high blood pressure to a normal level in hypertensive rats.

3.3. Hemolytic activity of MP-B and its D-isomers

Native MP-B possesses a potent hemolytic activity on the red blood cells of the guinea-pig and rat (Ho and Hwang, 1991; Ho et al., 1996). At a concentration of 15 μ M, more than 85% of the guinea-pig red cells were lysed by the peptides, and complete hemolysis ($>95\%$) was achieved at a concentration of 20 μ M (Fig. 4). Substitution of Lys²

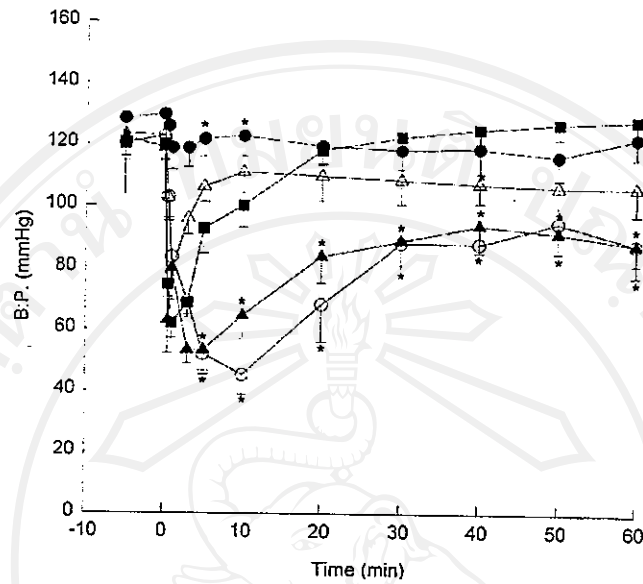


Fig. 2. Hypotensive effect of MP-B and its D-isomers in the rat. MP-B (■), D-MP-B (○), [D-Lys²]MP-B (●), [D-Lys⁴]MP-B (△) or [D-Lys¹¹,¹²]MP-B (▲) was injected via the femoral vein at a dose of 0.5 mg/kg at zero time. Mean blood pressure (B.P.) was measured as described in Materials and Methods. Each point represents mean \pm SEM of three to four animals. * P < 0.05 as compared with MP-B at corresponding time (5–60 min).

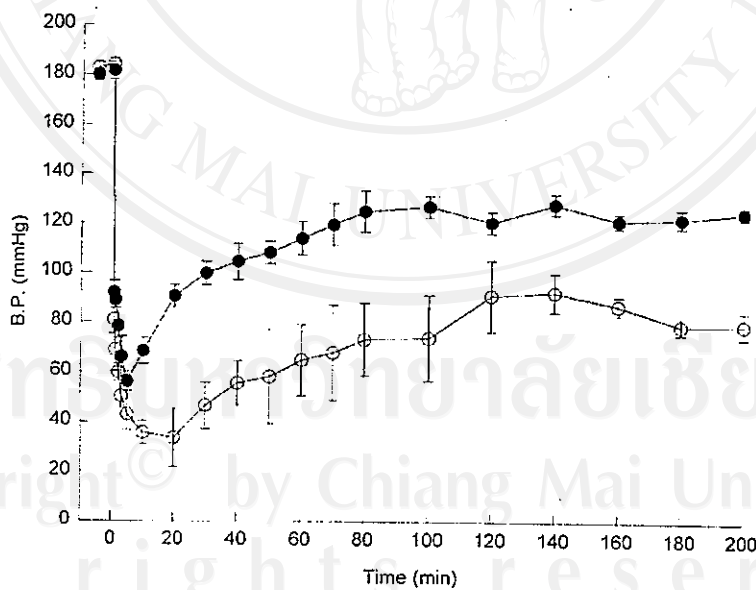


Fig. 3. Hypotensive effect of [D-Lys¹¹,¹²]MP-B on spontaneously hypertensive rats. [D-Lys¹¹,¹²]MP-B was injected via the femoral vein at doses of 0.3 (●) and 0.5 (○) mg/kg at zero time. Mean blood pressure (B.P.) was measured as described in the materials and methods section. Each point represents mean \pm SEM of three to four animals. Note that a dose of 0.3 mg/kg peptide can lower and maintain the blood pressure of the SHR rats at about 120 mm Hg for more than 3 h.

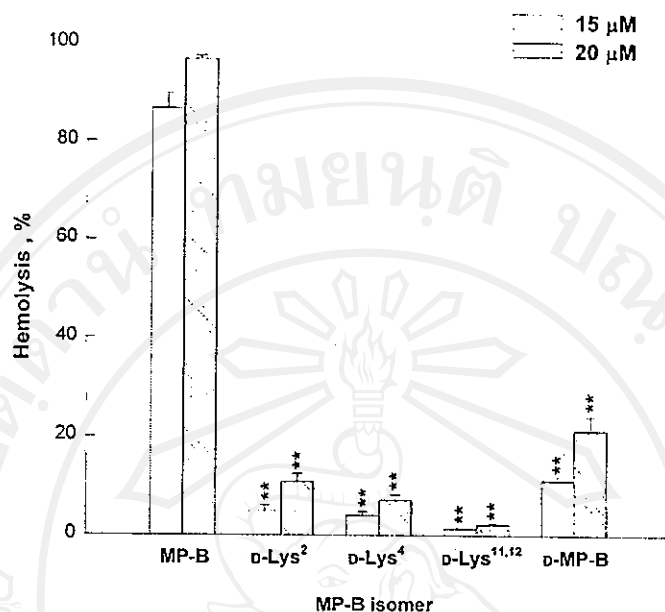


Fig. 4. Hemolytic activity of MP-B and its D-isomers. Direct hemolytic activity of MP-B and its isomers was assayed on washed red blood cells of the guinea-pig. The red blood cells (1%) were incubated with the peptides (15 and 20 μ M) in Tris-buffered (0.01 M, pH 7.4) saline at 37°C for 60 min. Data shown are mean \pm SEM from six experiments. ** P < 0.01 as compared with MP-B at the corresponding concentration.

by D-Lys in MP-B caused about 90% decrease in its hemolytic activity, while replacement of Lys⁴ or Lys^{11,12} by D-Lys almost abolished the hemolytic activity of MP-B (Fig. 4). No significant hemolysis (<5%) was found with [D-Lys^{11,12}]MP-B even when the peptide concentration was increased to 30 μ M. D-MP-B in which all residues are substituted by D-amino acids showed a hemolytic activity about 1/5 that of L-isomer.

4. Discussion

The present study on the hypotensive and hemolytic activities of D-isomers of MP-B has shown that the substitution of Lys² by D-Lys in MP-B caused a significant decrease in both the hemolytic and hypotensive activities of MP-B. The substitution of Lys⁴ by D-Lys in MP-B caused a great reduction of the hemolytic activity, but its hypotensive activity was only slightly affected. However, when Lys^{11,12} were replaced by D-Lys, the D-isomer showed a marked increase in its hypotensive activity while its hemolytic activity was almost abolished. The all-D isomer of MP-B showed the highest hypotensive activity with a hemolytic activity about 1/5 that of MP-B. These results indicate that D-Lys substitution carried out at N-terminus of MP-B (Lys^{2,4}) causes a decrease in both the hypotensive and hemolytic activities, while the substitution at C-terminus

(Lys^{11,12}) by D-Lys causes an increase in hypotensive activity of MP-B with salient decrease in hemolytic activity. [D-Lys^{11,12}] MP-B (0.3 mg/kg) effectively lowers and maintains the blood pressure of spontaneously hypertensive rats at a normal level for several h. [D-Lys^{11,12}] MP-B, which showed a higher hypotensive activity with the least hemolytic side effect, appears to be the best MP-B analog for studying the hypotensive mechanism of MP-B and could be useful as a hypotensive agent for research or as a therapeutic agent in hypertension crisis.

Mastoparan B exhibited a CD spectrum rich in α -helix conformation in Tris-buffered saline containing 20% trifluoroethanol (Ilo et al., 1996; Chuang et al., 1996). In a preliminary study on the CD spectra of MP-B and its D-isomers, we have found that the substitution of Lys² by D-Lys in MP-B caused little change in its conformation with significant decrease in hemolytic and hypotensive activities, while D-Lys substitution at Lys^{11,12} of MP-B caused a drastic change in the CD spectrum with increased hypotensive and decreased hemolytic activities. It appears that the changes of biological activities by D-amino acid substitution in MP-B sequence are not consistent with the conformational changes of the peptide resulting from backbone alteration. The finding that D-Lys substituted MP-B isomers nearly lose their hemolytic activity indicates that lytic action of MP-B requires a rather restrictive configuration of the Lys residues. The enhancement of hypotensive effect of

MP-B by D-Lys substitution at the C-terminus (Lys^{11,12}) suggests that trypsin-like enzymes, preferring to cleave the L-proteins or peptides with a Lys-Lys-X motif in the C-terminal region, may be involved in regulating the duration of MP-B action in vivo. Our contention is consistent with the earlier finding that a trypsin-like enzyme, tryptase, is released from mast cells when the cells are stimulated (Irani et al., 1986; Thomas et al., 1998).

Acknowledgements

We are grateful to Dr Guor-Rong Her for his kind assistance in determining the molecular mass of MP-B and its isomers. This work was supported by grants from the National Science Council and Academia Sinica, Taipei, Taiwan, Republic of China.

References

- Chuang, C.C., Huang, W.C., Yu, H.M., Wang, K.T., Wu, S.H., 1996. Conformation of *Vespa basalis* mastoparan-B in trifluoroethanol-containing aqueous solution. *Biochim. Biophys. Acta* 1292, 1–8.
- Ho, C.L., Hwang, L.L., 1991. Structure and biological activities of a new mastoparan isolated from the venom of the hornet *Vespa basalis*. *Biochem. J.* 274, 453–456.
- Ho, C.L., Hwang, L.L., Lin, Y.L., Chen, C.T., Yu, H.M., Wang, K.T., 1994. Cardiovascular effects of mastoparan B and its structural requirements. *Eur. J. Pharmacol.* 259, 259–264.
- Ho, C.L., Lin, Y.L., Chen, W.C., Hwang, L.L., Yu, H.M., Wang, K.T., 1996. Structural requirements for the edema-inducing and hemolytic activities of mastoparan B isolated from the hornet (*Vespa basalis*) venom. *Toxicon* 34, 1027–1035.
- Irani, A.A., Schechter, N.M., Craig, S.S., DeBlois, G., Schwartz, L.B., 1986. Two types of human mast cells that have distinct neutral protease compositions. *Proc. Natl. Acad. Sci. USA* 83, 4464–4468.
- Nakajima, T., 1984. Biochemistry of vespid venoms. In: Tu, A.T. (Ed.), *Handbook of Natural Toxins*, Vol. 2. Marcel Dekker, New York, pp. 109–133.
- Nakajima, T., 1986. Pharmacological biochemistry of vespid venoms. In: Pick, T. (Ed.), *Venom of Hymenoptera*. Academic Press, London, pp. 309–327.
- Pick, T., 1984. Pharmacology of hymenoptera venom. In: Tu, A.T. (Ed.), *Handbook of Natural Toxins*, Vol. 2. Marcel Dekker, New York, pp. 135–185.
- Thomas, V.A., Wheelless, C.J., Staek, M.S., Johnson, D.A., 1998. Human mast cell tryptase fibrinogenolysis: kinetics, anticoagulation mechanism, and cell adhesion disruption. *Biochemistry* 37, 2291–2298.
- Wu, S.H., Wang, K.T., Ho, C.L., 1982. Purification and pharmacological characterization of a cardiotoxin-like protein from Formosan banded krait (*Bungarus multicinctus*) venom. *Toxicon* 20, 753–764.
- Yu, H.M., Wu, T.M., Chen, S.T., Ho, C.L., Her, G.R., Wang, K.T., 1993. Mastoparan B: synthesis and its physical and biological properties. *Biochem. Mol. Biol. Int.* 29, 241–246.

VITA

Name: HUI-MING YU (Mrs.)

Date of Birth: 29. Nov. 1960

Work address:

Institute of Biological Chemistry, Academia Sinica

128, Yun-Chir-Yuan Road, Sec. 2, Nankang, Taipei 11529, Taiwan

TEL: +886-2-27855696 ext. 4110

FAX: +886-2-27835945

E-mail: hmyu@gate.sinica.edu.tw

Education :

1981-1986 B.Sc. (Pharmacology), Taipei Medical College, Taipei, Taiwan

1998-2004 Ph.D. (Biotechnology), Faculty of Science, Chiang Mai University,
Chiang Mai, Thailand

Experiential work

1986-present Research technician, Academia Sinica

Awards

1999 An exemplary person of Academia Sinica

2000-2002 An advisory counselor of DigitalGene Biosciences Co., Ltd.

2002-present An advisory counselor of HsinChan Co.,

Published papers :

1. Yu, H.M., Chen, S.T., Chen, S.W., Ko, J.L. and Wang, K.T. (1987) The synthesis of dermorphin derivatives. *J. Chinses Biochem. Soc.* 16, 61-69.
2. Yu, H.M., Chen, S.T., Chior, S.H. and Wang, L.T. (1988) Determination of amino acids on merrifield resin by microwave hydrolysis. *J. Chromatog.* 456, 357-362.
3. Wu, C.Y., Chen, W.C., Yu, H.M., Chen, S.T. and Wang, K.T. (1992) Side reaction in peptide synthesis: failure coupling in solid phase automatic synthesis of a fragment (sequence 65-74) of acyl carrier protein. *J. Chinese Chem. Soc.* 39, 195-198.
4. Yu, H.M., Chen, S.T. and Wang, K.T. (1992) Enhanced coupling efficiency in solid-phase peptide by microwave irradiation. *J. Org. Chem.* 57, 4780-4784.
5. Yu, H.M., Wu, T.M., Chen, S.T., Ho, C.L., Her, G.R. and Wang, K.T. (1993) Mastoparan-B, synthesis and its physical and biological properties. *Biochem. & Molecular Biolog. Intermal.* 29(2), 241-246.
6. Chen, S.T., Chem, H.J., Yu, H.M. and Wang, K.T. (1993) Facile synthesis of a short peptide with a side-chain constrained structure. *J. Chem. Research* 6, 228-229.
7. Ho, C.L., Hwang, L.L., Lin, Y.L., Chen, S.T., Yu, H.M. and Wang, K.T. (1994) Cardiovascular effects of mastoparan-B and its structural requirements. *Eur. J. Pharmacol.* 259, 259-264.
8. Jayaraman, G., Bhaskaran, R., Kumar, T.K.S., Yu, H.M., Chen, S.T. and Yu, C. (1995) Conformational studies of a synthetic cyclic decapeptide fragment of rat transforming growth factor- α . *Int, J, Peptide Protein Res.* 46, 88-96.

9. Ho, C.L., Lin, Y.L., Chen, W.C., **Yu, H.M.**, Wang, K.T., Hwang, L.L. and Chen, S.T. (1995) Immunogenicity of mastoparan-B, a cationic tetradecapeptide isolated from the hornet (*Vespa basalis*) venom, and its structural requirements. *Toxicon*, 33, 1443-1451.
10. Chuang, C.C., Huang, W.C., **Yu, H.M.**, Wang, K.T. and Wu, S.H. (1996) Conformation of vespa basalis mastoparan-B in trifluoroethanol-containing aqueous solution. *Biochimica. Biophys. Acta* 1292, 1-8.
11. Chuang, L.C., **Yu, H.M.**, Chen, C., Huang, T.H., Wu, S.H. and Wang, K.T. (1996) Determination of three-dimensional solution structure of waglerin I, a toxin from *Trimeresurus wagleri*, using 2D-NMR and molecular dynamics simulation. *Biochim. Biophys. Acta* 1292, 145-155.
12. Ho, C.L., Lin, Y.L., Chen, W.C., Hwang, L.L., **Yu, H.M.** and Wang K.T. (1996) Structural requirements for the edema-inducing and hemolytic activities of mastoparan B isolated from the hornet (*Vespa Basalis*) Venom. *Toxicon*, 34, 1027-1035.
13. Hsiao, Y.M., Chuang, C.C., Chuang, L.C., **Yu, H.M.**, Wang, K.T., Chior, S.H. and Wu, S.H. (1996) Protein engineering of venom toxins by synthetic approach and NMR dynamic simulation: status of basic amino acid residues in waglerin I. *Biochem. Biophys. Res. Comm.* 227, 59-63.
14. **Yu, H.M.**, Chen, S.T., Phutrakul, S., Rakariyatham, N. and Wang, K.T. (1996) The effect of microwave irradiation on acid-catalyzed hydrolysis of starch. *J. Org.Chem.* 61, 9608-9610.

15. Chen, S.T., Tseng, P.H., **Yu, H.M.**, Wu, C.Y., Hsiao, K.F., Wu, S.H. and Wang, K.T. (1997) The studies of microwave effects on the chemical reactions. *J. Chin. Chem. Soc.* 44, 169-182.
16. Wu, Y.T., Hsieh, H.P., Wu, C.Y., **Yu, H.M.**, Chen, S.T. and Wang, K.T. (1998) Facile solid phase synthesis of octreotide analogs using p-carboxybenzaldehyde as a novel linker to anchor Fmoc-threoninol to solid phase resins. *Tetrahedron Lett.* 39, 1783-1784.
17. **Yu, H.M.**, Chen, S.T., Tseng, M.J., Chen, S.T. and Wang, K.T. (1999) Microwave-assisted heterogeneous Benzil-Benzilic acid rearrangement. *J. Chem. Res. S.* 62-63.
18. Chen, S.T., **Yu, H.M.**, and Wang, K.T. (1999) Microwave-assisted solid reaction: Reduction of ketones using sodium borohydride. *J. Chin. Chem. Soc.* 46, 509-511.
19. **Yu, H.M.**, Lin, H.L., Wu, C.Y., Tseng, M.J. and Chen, S.T. (1999) Enzymatic reaction in supercritical fluid carbon dioxide using dry-ice. *J. Chin. Chem. Soc.* 46, 647-650.
20. Ho, C.L., Shih, Y.P., Wang, K.T. and **Yu, H.M.** (2001) Enhancing the hypotensive effect and diminishing the cytolytic activity of hornet mastoparan B by D-amino acid substitution. *Toxicon* 39, 1561-1566.
21. Lee, Y.C., Lin, S.D., **Yu, H.M.** and Chen, S.T. (2001) Phosphorylation of the 24p3 protein secreted from mouse uterus *in vitro* and *in vivo*. *J. Protein Chem.* 20, 563-569.
22. Wang, I., Wu, S.H., Chang, H.K., Shieh, R.C., **Yu, H.M.** and Chen, C. (2002) Solution Structure of a K-Channel Blocker from the Scorpion *Tityus cambridgei*. *Protein Sci.* 389-400.

23. Babu, G., **Yu, H.M.**, Yang, S.M. and Fang, J.M. (2004) Carbazolothiophene-2-carboxylic acid derivatives as endothelin receptor antagonists. *Bioorg. Med. Chem. Lett.* 14, 1129-1132.
24. **Yu, H.M.**, Tseng, M.J., Fang, J.M., Phutrakul, S. and Chen, S.T. (2004) Capillary electrophoresis using immobilized whole cells with overexpressed endothelin receptor for specific ligand screening. *Electrophoresis* 25, 1034-1041.

Conference papers :

1. Wang, K.T., **Yu, H.M.**, Chen, S.T. and Ho, C.L. (1994) Isolation of a hypoglycaemic factor from wheat green. First APSB International Symposium and Workshop, Singapore, Aug. 15-18.
2. **Yu, H.M.**, Chen, S.T., Ho, C.L. and Wang, K.T. (1995) Isolation of a hypoglycaemic factor from wheat green. Czech-Taiwan Symposium on Biotechnology, Prague, June 5-8.
3. **Yu, H.M.**, Hsiao, K.F., Chen, S.T. and Wang, K.T. (1996) Rate-enhanced of enzyme-catalysis by microwave irradiation. International Symposium Organic Reactions-Sendai, Sendai, Japan, April 6-9.
4. **Yu, H.M.**, Chen, S.T., Phutrakul, S., Rakariyatham, N. and Wang, K. T. (1996) Effects of microwave irradiation on the acid-catalyzed hydrolysis of starch. International Conference in Glycobiology, Taipei, Taiwan, November 15-16.
5. **Yu, H.M.**, Tseng, P.H., Wu, C.Y., Hsiao, K.F., Wu, S.H., Chen, S.T. and Wang, K.T. (1998) Microwave enhanced chemical reactions. International Conference on Microwave Chemistry, Prague, Czech Republic, September 6-11.